

2

# NAVAL POSTGRADUATE SCHOOL

Monterey, California

AD-A247 034



DTIC  
ELECTE  
MAR 04 1992  
S D D

## THESIS

PERFORMANCE OF A FAST FREQUENCY-HOPPED  
NONCOHERENT MFSK RECEIVER WITH RATIO-STATISTIC  
COMBINING OVER RICIAN FADING CHANNELS WITH  
PARTIAL-BAND INTERFERENCE

by

John F. Riley

June, 1991

Thesis Advisor:  
Thesis Co-Advisor:

R. Clark Robertson  
Tri T. Ha

Approved for public release; distribution is unlimited

92 3 02 054

92-05294



REPORT DOCUMENTATION PAGE				
1a. REPORT SECURITY CLASSIFICATION UNCLASSIFIED			1b. RESTRICTIVE MARKINGS	
2a. SECURITY CLASSIFICATION AUTHORITY			3. DISTRIBUTION/AVAILABILITY OF REPORT Approved for public release; distribution is unlimited.	
2b. DECLASSIFICATION/DOWNGRADING SCHEDULE				
4. PERFORMING ORGANIZATION REPORT NUMBER(S)			5. MONITORING ORGANIZATION REPORT NUMBER(S)	
6a. NAME OF PERFORMING ORGANIZATION Naval Postgraduate School		6b. OFFICE SYMBOL (If applicable) EC		7a. NAME OF MONITORING ORGANIZATION Naval Postgraduate School
6c. ADDRESS (City, State, and ZIP Code) Monterey, CA 93943-5000			7b. ADDRESS (City, State, and ZIP Code) Monterey, CA 93943-5000	
8a. NAME OF FUNDING/SPONSORING ORGANIZATION		8b. OFFICE SYMBOL (If applicable)		9. PROCUREMENT INSTRUMENT IDENTIFICATION NUMBER
8c. ADDRESS (City, State, and ZIP Code)			10. SOURCE OF FUNDING NUMBERS	
			Program Element No	Project No
			Task No	Work Unit Accession Number
11. TITLE (Include Security Classification) PERFORMANCE OF A FAST FREQUENCY-HOPPED NONCOHERENT MFSK RECEIVER WITH RATIO-STATISTIC COMBINING OVER RICIAN FADING CHANNELS WITH PARTIAL-BAND INTERFERENCE				
12. PERSONAL AUTHOR(S) Riley, John F.				
13a. TYPE OF REPORT Master's Thesis		13b. TIME COVERED From To		14. DATE OF REPORT (year, month, day) 1991 June
15. PAGE COUNT 105				
16. SUPPLEMENTARY NOTATION The views expressed in this thesis are those of the author and do not reflect the official policy or position of the Department of Defense or the U.S. Government.				
17. COSATI CODES			18. SUBJECT TERMS (continue on reverse if necessary and identify by block number)	
FIELD	GROUP	SUBGROUP	Ratio-Statistic Combining; Fast Frequency-Hopping; Rician Fading; FSK Modulation; Partial-Band Interference	
19. ABSTRACT (continue on reverse if necessary and identify by block number)				
<p>An error probability analysis is performed for a fast frequency-hopped, frequency-shift keyed noncoherent receiver with ratio-statistic combining for a Rician channel with partial-band interference. Results are obtained for binary and M-ary FSK receivers where M is 4, 8, or 16. Both envelope and square-law detectors were analyzed.</p> <p>The probability of bit error is examined for different levels of diversity, thermal noise, severity of fading, fractions of bandwidth jammed, and varying jamming power. Comparisons for the different parameters are done to determine when diversity should be used.</p> <p>For the special case when there is no diversity, an analytic expression for receiver performance is obtained, and the performance of a receiver using envelope detection is found to be identical to that of a receiver using square-law detection for this special case. The results show that, for diversities of three and four, the envelope detector performs better than the square-law detector.</p> <p>It is shown that, for low bit energy-to-jammer density ratios, diversity is generally a disadvantage, and for high bit energy-to-jammer density ratios, diversity is generally an advantage. The transition is dependent on thermal noise and the value of M.</p>				
20. DISTRIBUTION/AVAILABILITY OF ABSTRACT			21. ABSTRACT SECURITY CLASSIFICATION	
<input checked="" type="checkbox"/> UNCLASSIFIED/UNLIMITED <input type="checkbox"/> SAME AS REPORT <input type="checkbox"/> DTIC USERS			UNCLASSIFIED	
22a. NAME OF RESPONSIBLE INDIVIDUAL Robertson, R. Clark			22b. TELEPHONE (Include Area code) 408-646-2382	22c. OFFICE SYMBOL EC/Rc

Approved for public release; distribution is unlimited.

Performance of a Fast Frequency-Hopped Noncoherent MFSK Receiver with  
Ratio-Statistic Combining over Rician Fading Channels with Partial-Band  
Interference

by

John F. Riley  
Lieutenant, U.S.N.  
B.S. in E.E., The Citadel, 1985

Submitted in partial fulfillment  
of the requirements for the degree of

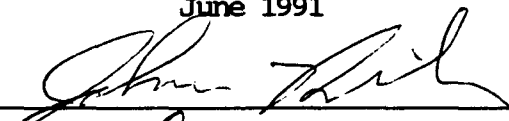
MASTER OF SCIENCE IN ELECTRICAL ENGINEERING  
(SPACE SYSTEMS ENGINEERING)

from the

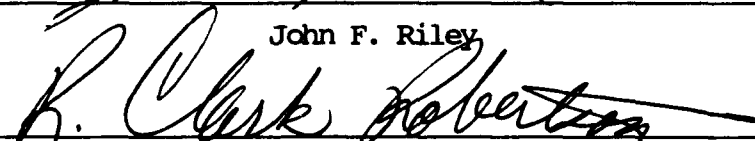
NAVAL POSTGRADUATE SCHOOL


June 1991


Author:

  
\_\_\_\_\_  
John F. Riley

Approved by:

  
\_\_\_\_\_  
R. Clark Robertson, Thesis Advisor

  
\_\_\_\_\_  
Tri T. Ha, Thesis Co-Advisor

  
\_\_\_\_\_  
Michael A. Morgan, Chairman  
Department of Electrical and Computer Engineering

## ABSTRACT

An error probability analysis is performed for a fast frequency-hopped, frequency-shift keyed noncoherent receiver with ratio-statistic combining for a Rician channel with partial-band interference. Results are obtained for binary and  $M$ -ary FSK receivers where  $M$  is 4, 8, or 16. Both envelope and square-law detectors were analyzed.

The probability of bit error is examined for different levels of diversity, thermal noise, severity of fading, fractions of bandwidth jammed, and varying jamming power. Comparisons for the different parameters are done to determine when diversity should be used.

For the special case when there is no diversity, an analytic expression for receiver performance is obtained, and the performance of a receiver using envelope detection is found to be identical to that of a receiver using square-law detection for this special case. The results show that, for diversities of three and four, the envelope detector performs better than the square-law detector.

It is shown that, for low signal-to-jammer ratios, diversity is generally a disadvantage, and for high signal-to-jammer ratios, diversity is generally an advantage. The transition is dependent on thermal noise and the value of  $M$ .



Accession For	
NTIS CRA&I	<input checked="checked" type="checkbox"/>
DTIC TAB	<input type="checkbox"/>
Unannounced	<input type="checkbox"/>
Justification	
By	
Distribution /	
Availability Codes	
Dist	Avail and/or Special
A-1	

## TABLE OF CONTENTS

I.	INTRODUCTION . . . . .	1
II.	SYSTEM DESCRIPTION . . . . .	6
A.	SPREAD SPECTRUM . . . . .	6
1.	Time-Hopped Spread Spectrum . . . . .	6
2.	Direct Sequence Spread Spectrum . . . . .	7
3.	Frequency-Hopped Spread Spectrum . . . . .	10
B.	FREQUENCY SHIFT KEYING (FSK) . . . . .	15
1.	Envelope Detector . . . . .	18
2.	Square-Law Detector . . . . .	19
C.	Partial-Band Jamming . . . . .	19
D.	Rician Fading . . . . .	20
E.	RATIO-STATISTIC COMBINING . . . . .	24
III.	MATHEMATICAL ANALYSIS . . . . .	27
A.	INITIAL GOALS OF DERIVATION . . . . .	27
B.	BFSK ENVELOPE DETECTOR . . . . .	31
1.	Forming the Joint Density Function . . . . .	32
2.	Setting Up The Auxiliary Variable . . . . .	32
3.	The Joint Density Theorem . . . . .	34
4.	Integrating Out The Auxiliary Variable . . . . .	36
5.	Adding Rician Fading . . . . .	36

6. Final Probability Density Functions . . . . .	37
C. BFSK SQUARE-LAW DETECTOR . . . . .	38
1. Forming the Joint Density Function . . . . .	39
2. Finding $f_{y_1}(y_1)$ . . . . .	40
3. Final Probability Density Functions . . . . .	41
D. Special Case For $L=1$ . . . . .	42
1. Envelope Detector . . . . .	43
2. Square Law Detector . . . . .	45
E. M-ARY FSK DERIVATION . . . . .	47
1. Union Bound . . . . .	49
2. Converting From Bit Error to Symbol Error . . . . .	51
F. PROBABILITY OF BIT ERROR . . . . .	52
IV. NUMERICAL RESULTS . . . . .	54
A. NUMERICAL PROCEDURE . . . . .	54
B. BFSK ENVELOPE DETECTOR . . . . .	57
1. $E_b/N_o = 16$ dB . . . . .	57
2. $E_b/N_o = 13.35$ dB . . . . .	66
C. M-ARY ENVELOPE DETECTOR . . . . .	77
D. ENVELOPE DETECTOR VERSUS SQUARE-LAW DETECTOR . . . . .	90
V. CONCLUSIONS . . . . .	100
INITIAL DISTRIBUTION LIST . . . . .	104

## LIST OF FIGURES

Figure 2.1: Time-Hopping Spread Spectrum . . . . .	7
Figure 2.2: Direct Sequence Spread Spectrum . . . . .	9
Figure 2.3: Direct Sequence Spread Spectrum Transmitter . . . . .	10
Figure 2.4: Frequency Hopping Spread Spectrum . . . . .	11
Figure 2.5: Frequency Hopping Transmitter . . . . .	12
Figure 2.6: Frequency Hopping Receiver . . . . .	14
Figure 2.7: M-ARY FSK . . . . .	16
Figure 2.8: BFSK Receiver . . . . .	17
Figure 2.9: Envelope Detection Of A Sine Wave . . . . .	18
Figure 2.10: Partial-Band Jamming . . . . .	20
Figure 2.11: Geosynchronous Satellite to Fixed Ground Terminal Link. . . . .	21
Figure 2.12: Mobile-To-Mobile Ground Link . . . . .	22
Figure 2.13: Low Earth Orbit to Mobile Ground Terminal Link. . . . .	23
Figure 2.14: Block Diagram for a Receiver Employing Ratio-Statistic Combining. . . . .	26
Figure 3.1. Alternate Implementation of the Ratio-Statistic Receiver. . . . .	28
Figure 3.2: M-ary FSK Receiver . . . . .	48
Figure 4.1: $f_{y_1}(y_1)$ where $E_b/N_0=13.35\text{dB}$ , $E_b/N_j=20\text{dB}$ , Direct/Diffuse=10, $\gamma=.25$ . . . . .	55

Figure 4.2: $f_{y_1}(y_1)$ where $E_b/N_0=13.35\text{dB}$ , $E_b/N_j=3\text{dB}$ , Direct/Diffuse=10, $\gamma=.25$ . . . . .	56
Figure 4.3: Probability of Bit Error Versus Direct-to-Diffuse Ratio for a BFSK Receiver with Envelope Detection where $E_b/N_0=16\text{dB}$ , No Jamming . . . . .	58
Figure 4.4: Performance of a BFSK Receiver with Envelope Detection where $E_b/N_0=16\text{dB}$ , Direct/Diffuse=10, and $L=1$ . . . . .	60
Figure 4.5: Performance of a BFSK receiver with Envelope Detection where $E_b/N_0=16\text{dB}$ , Direct/Diffuse=10, and $L=2$ . . . . .	61
Figure 4.6: Performance of a BFSK Receiver with Envelope Detection where $E_b/N_0=16\text{dB}$ , Direct/Diffuse=10, and $L=3$ . . . . .	62
Figure 4.7: Performance of a BFSK Receiver with Envelope Detection where $E_b/N_0=16\text{dB}$ , Direct/Diffuse=10, and $L=4$ with $L=1$ worst case . . . . .	63
Figure 4.8: Performance of a BFSK Receiver with Envelope Detection where $E_b/N_0=16\text{dB}$ , Direct/Diffuse=10000, and $L=1$ . . . . .	67
Figure 4.9: Worst Case Performance of a BFSK Receiver with Envelope Detection where $E_b/N_0=16\text{dB}$ , Direct/Diffuse=.01, and $L=1, 2, 3$ and 4. . . . .	68
Figure 4.10: Worst Case Performance of a BFSK Receiver with Envelope Detection where $E_b/N_0=16\text{dB}$ and $L=4$ for Different Amounts of Fading . . . . .	69



Figure 4.11: Performance of a BFSK Receiver with Envelope Detection where $E_b/N_0=13.35\text{dB}$ , Direct/Diffuse=10, and $L=1$ . . . . .	70
Figure 4.12: Performance of a BFSK Receiver with Envelope Detection where $E_b/N_0=13.35\text{dB}$ , Direct/Diffuse=10, and $L=2$ . . . . .	71
Figure 4.13: Performance of a BFSK Receiver with Envelope Detection where $E_b/N_0=13.35\text{dB}$ , Direct/Diffuse=10, and $L=3$ . . . . .	72
Figure 4.14: Performance of a BFSK Receiver with Envelope Detection where $E_b/N_0=13.35\text{dB}$ , Direct/Diffuse=10, and $L=4$ with $L=1$ worst case . . . . .	73
Figure 4.15: Performance of a BFSK Receiver with Envelope Detection where $E_b/N_0=13.35\text{dB}$ , Direct/Diffuse=10000, and $L=1$ and 4. . . . .	74
Figure 4.16: Comparison of the Performance of a BFSK Receiver with Envelope Detection where Direct/Diffuse=10 for $E_b/N_0=13.35\text{dB}$ versus 16dB . .	76
Figure 4.17: Worst Case Performance of a 4-ary FSK Receiver with Envelope Detection where $E_b/N_0=16\text{dB}$ , Direct/Diffuse=10, and $L=1$ and 4 . . . . .	78
Figure 4.18: Worst Case Performance of an 8-ary FSK Receiver with Envelope Detection where $E_b/N_0=16\text{dB}$ , Direct/Diffuse=10, and $L=1$ and 4 . . . . .	79

<b>Figure 4.19: Worst Case Performance of a 16-ary FSK Receiver with Envelope Detection where <math>E_b/N_0=16\text{dB}</math>, Direct/Diffuse=10, and <math>L=1</math> and 4 . . . . .</b>	<b>80</b>
<b>Figure 4.20: Worst Case Performance of a 4-ary FSK Receiver with Envelope Detection where <math>E_b/N_0=16\text{dB}</math>, Direct/Diffuse=.01, and <math>L=1-4</math> . . . . .</b>	<b>81</b>
<b>Figure 4.21: Worst Case Performance of an 8-ary FSK Receiver with Envelope Detection where <math>E_b/N_0=16\text{dB}</math>, Direct/Diffuse=.01, and <math>L=1-4</math> . . . . .</b>	<b>82</b>
<b>Figure 4.22: Worst Case Performance of a 16-ary FSK Receiver with Envelope Detection where <math>E_b/N_0=16\text{dB}</math>, Direct/Diffuse=.01, and <math>L=1-4</math> . . . . .</b>	<b>83</b>
<b>Figure 4.23: Performance of a 4-ary FSK Receiver with Envelope Detection where <math>E_b/N_0=16\text{dB}</math>, Direct/Diffuse=10, and <math>L=4</math> . . . . .</b>	<b>85</b>
<b>Figure 4.24: Performance of M-ary FSK Receivers with Envelope Detection where <math>E_b/N_0=16\text{dB}</math>, Direct/Diffuse=10, <math>L=4</math> and <math>M=2, 4, 8</math>, and 16 . . .</b>	<b>86</b>
<b>Figure 4.25: Performance of an 8-ary FSK Receiver with Envelope Detection where <math>E_b/N_0=16\text{dB}</math>, Direct/Diffuse=10000, and <math>L=4</math> . . . . .</b>	<b>87</b>
<b>Figure 4.26: Performance of a 4-ary FSK Receiver with Envelope Detection where <math>E_b/N_0=16\text{dB}</math>, Direct/Diffuse=10 for <math>E_b/N_0=13.35</math> versus 16dB . . . . .</b>	<b>88</b>

Figure 4.27: Performance of BFSK Receiver with $L=4$ versus M-ary Receivers with $L=1$ where $E_b/N_0=16\text{dB}$ , Direct/Diffuse=.01 and Envelope Detection . . . . .	91
Figure 4.28: Performance of a BFSK Receiver with $L=4$ versus M-ary Receivers with $L=1$ where $E_b/N_0=16\text{dB}$ , Direct/Diffuse=10 and Envelope Detection . . . . .	92
Figure 4.29: Performance of a BFSK Receiver with $L=4$ versus M-ary Receivers with $L=1$ where $E_b/N_0=13.35\text{dB}$ , Direct/Diffuse=10 and Envelope Detection . . . . .	93
Figure 4.30: Performance of a BFSK Receiver with $L=4$ versus M-ary Receivers with $L=1$ where $E_b/N_0=16\text{dB}$ , Direct/Diffuse=10000 and Envelope Detection . . . . .	94
Figure 4.31: $f_{y_1}(y_1)$ where $E_b/N_0=13.35\text{dB}$ , $E_b/N_j=20\text{dB}$ , Direct/Diffuse=10, and $\gamma=.25$ with Square-Law Detection . . . . .	96
Figure 4.32: $f_{y_1}(y_1)$ where $E_b/N_0=13.35\text{dB}$ , $E_b/N_j=3\text{dB}$ , Direct/Diffuse=10, and $\gamma=.25$ with Square-Law Detection . . . . .	97
Figure 4.33: Envelope Detector versus Square-Law Detector Worst Case Performance for BFSK Receivers where $E_b/N_0=16\text{dB}$ , Direct/Diffuse=10 . . . . .	98
Figure 4.34: Envelope Detector Performance versus Square- Law Detector Performance for BFSK Receivers where $E_b/N_0=13.35\text{dB}$ , Direct/Diffuse=10 . . . . .	99

## I. INTRODUCTION

More than two decades prior to the advent of the space program, Arthur C. Clarke realized the advantage of satellite communications systems [REF 1]. A satellite can orbit the earth and maintain a much wider field of view than a land based system and, therefore, cover a much larger area. For example, a ground terminal on the east coast of the United States can be in the same satellite footprint as a terminal on the west coast of the United States, and the two terminals can easily communicate by linking to the satellite. Even if the two terminals are not in the same footprint, it is a simple matter for one satellite to link to another for world wide communications.

With the advent of satellite communications, however, several problems came to light. One problem is that, since satellites have such a wide footprint, interference, both intentional and unintentional, is a problem. A satellite can be jammed simply by transmitting in the same bandwidth as the satellite. One method of overcoming this is to spread the satellite signal over a very wide frequency band so that it is less likely that enough power can be transmitted to jam the entire band. Spread-spectrum techniques spread the signal over a much wider bandwidth while transmitting the same amount

of power by transmitting with a pseudorandom pattern that is known only to friendly receivers.

Also, bandwidth is at a premium in the sense that there is a finite amount of frequency band to allocate to users and the lower frequency bands are already crowded. So frequency reuse plans have been adopted to conserve precious bandwidth. An alternative to frequency reuse is to design systems to operate in higher frequency ranges where more bandwidth is available. For example, the UHF band is from 300 MHz - 3 GHz and is already crowded. The EHF band is from 30-300 GHz and is not in great demand because of the higher free space and atmospheric losses associated with higher frequencies. If spread spectrum techniques are going to be used to their full advantage, it is likely that the EHF band will be exploited and losses in the channel are a great concern. Techniques have been developed to counteract these losses.

Many methods of cleverly coding the signal or using a special circuit in the receiver to conserve power or provide better reception have been developed. One such circuit that is designed to counteract the affects of partial-band jamming is known as a ratio-statistic combiner.

C. M. Keller and M. B. Pursley analyzed a ratio-statistic combining circuit in a frequency hopping spread spectrum system in the presence of partial-band interference for a channel with no fading [Ref 2]. They showed that improved performance is obtained by using the ratio-statistic combining

circuit. The spread spectrum scheme provides some immunity to jamming and interference, and the ratio-statistic combiner provides increased immunity to partial-band jamming.

The purpose of this thesis is to examine the performance of the ratio statistic combining circuit in a Rician fading channel for both a binary frequency-shift keyed (BFSK) and an  $M$ -ary frequency-shift keyed ( $M$ -ary FSK) system. Further discussion examines the actual amount of advantage in probability of bit error with particular attention to circumstances when the ratio-statistic combining circuit should not be used.

Before the analysis is discussed, a certain amount of ground work is laid. In Chapter II of the thesis, an overview of the system is given, beginning with a discussion of the different types of spread spectrum techniques and followed by a discussion of each step in the modulation and demodulation process before transmission and after reception.

The next focus in the thesis is the mathematical derivations and numerical analysis that are used to arrive at the results that appear later in the thesis. Particular attention is paid to the derivation of the probability density functions for both an envelope detector and a square-law detector in the BFSK receiver.

The later chapters discuss the results of the analysis and adapt the analysis to obtain a union bound for the more general  $M$ -ary case. Unlike a conventional  $M$ -ary FSK receiver,

an exact analysis of the  $M$ -ary FSK ratio-statistic receiver is not possible due to the nature of the receiver.

The conclusion of the thesis discusses the effect on performance of implementing diversity combined with the ratio-statistic receiver for various amounts of jamming and fading. Diversity combining is a method of increasing the redundancy of the information received discussed in Chapter II which improves performance up until the point where fading is low enough that the losses resulting from this more complex receiver will dominate the system and become a disadvantage. It is also expected that, as the number of symbols ( $M$ ) increases, there will be a noticeable increase in the performance of the system. The conclusion of the thesis discusses whether the results of the analysis support these expectations.

This thesis makes three assumptions regarding the channel. The first is that slow fading applies. Slow fading implies that the amplitude of the received signal remains constant at least during a hop and that the hop rate is much greater than the Doppler spread of the channel. This is a good assumption if the hop rate is fast. The second assumption is that the channel is frequency nonselective. If all frequency components in the signal bandwidth are affected in the same way by the channel, the channel is said to be frequency nonselective. This is a good assumption for lower data rates. The third assumption is that each hop fades independently.

That is, the smallest spacing between frequency hop slots for a bit is larger than the coherence bandwidth of the channel. These assumptions simplify the analysis of the system while maintaining good results.



## II. SYSTEM DESCRIPTION

### A. SPREAD SPECTRUM

Spread spectrum implies that the amount of bandwidth used to transmit the data is greater than necessary. Spread spectrum is used for several different reasons:

- provides some immunity to intentional jamming by forcing the jammer to spread his limited power over a wider bandwidth, thus reducing the jammer's effective power spectral density.
- creates confusion amongst conventional hostile receivers.
- allows for code-division multiple access (CDMA).
- encrypts the data for semi-secure communication.
- can provide accurate timing or ranging.
- provides covert communication by burying the signal below the thermal noise level.
- provides some protection from multi-path errors.

There are three basic types of spread spectrum: time-hopped, direct sequence, and frequency-hopped.

#### 1. Time-Hopped Spread Spectrum

In time-hopped spread spectrum communications, the period of a data bit is shortened significantly. Figure 2.1 is an illustration one bit of data. The larger block illustrates the period of the original data bit while the smaller bit shows the transmitted data as it would appear in time-hopping. For each data bit,  $t_1$  will vary within the

total period. Since the time-hopped data bit has a shorter period than the original data bit, it will have a higher bit rate and, therefore, a larger bandwidth. The increase in bandwidth is  $T/\tau$ , where  $T$  is the original bit period and  $\tau$  is the shorter bit period. Another way to describe this process is to say that the data is transmitted in bursts at pseudorandom times. Pseudorandom implies that the pattern is known to the friendly receiver but appears random to a hostile receiver. Time-hopping is not as practical as the other two spread spectrum techniques and is not used very often.

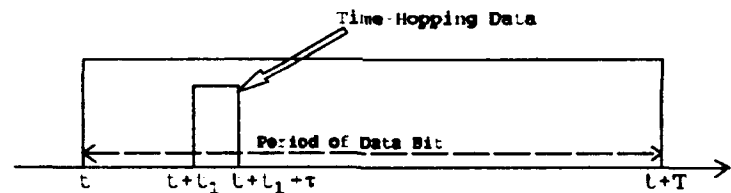


**Figure 2.1: Time-Hopping Spread Spectrum**

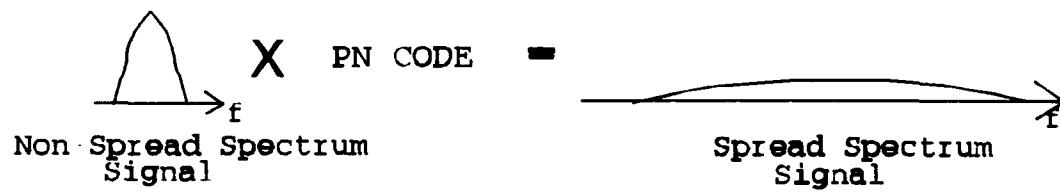
## **2. Direct Sequence Spread Spectrum**

In direct sequence spread spectrum, the data is modulated by a pseudo-noise (PN) code to spread the signal over a wider bandwidth. Figure 2.2 is an illustration of how the original signal, when multiplied (or mixed) with a PN

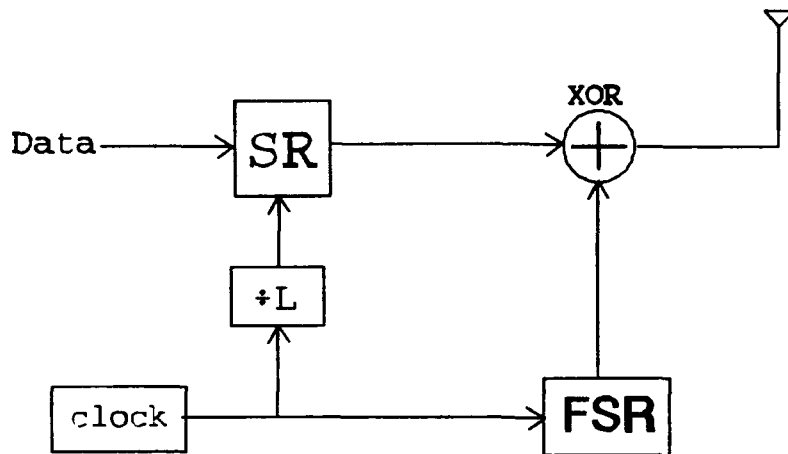
code, is spread out over a wider frequency band while transmitting the same total power.

Figure 2.3 is an illustration of a basic method of transmitting direct sequence spread spectrum. The clock in the circuit controls both the shift register (SR) and the feedback shift register (FSR). The FSR generates a PN code at the clock rate. The SR controls the flow of data to the exclusive-or (XOR) adder at the clock rate divided by  $L$ , where  $L$  is the length of the PN code. The result is that, for each data bit, either the full PN code or the inverse of the PN code is transmitted at a bit rate  $L$  times the data rate depending on whether a '1' or a '0' is to be transmitted, respectively.

In the receiver, the signal is mixed with the PN code once again in order to collapse the received signal back down to the original data signal. The receiver must know the PN code in order to correctly reproduce the data. The advantages of direct sequence are that it carries a certain amount of immunity to jamming, the transmission can be made covert by spreading the signal until it is buried below the noise level, the signal is encrypted by the PN code, and code division multiple access (CDMA) can be applied in order to increase channel capacity by assigning different PN codes to multiple users.



**Figure 2.2: Direct Sequence Spread Spectrum**



**Figure 2.3: Direct Sequence Spread Spectrum Transmitter**

### **3. Frequency-Hopped Spread Spectrum**

Frequency hopped spread spectrum is a technique where the information signal retains the same bandwidth but is hopped from one carrier frequency to another so that the transmitted signal fills a wider bandwidth. This is accomplished by the use of a hop pattern that moves the signal among the many carrier frequencies. The receiver must know the hop pattern in order to decode the signal in real time.

Figure 2.4 is an illustration of a basic frequency-hopped scheme. The blocks represent the information. At each time

the signal hops to a different carrier frequency based on a hop pattern that is related to the previously discussed PN code. In Figure 2.4, the hop pattern is repeating every seventh hop. This implies that a FSR with three registers is being used to generate the pattern since the length of the code is  $2^N - 1$  where  $N$  is the number of registers in the FSR.

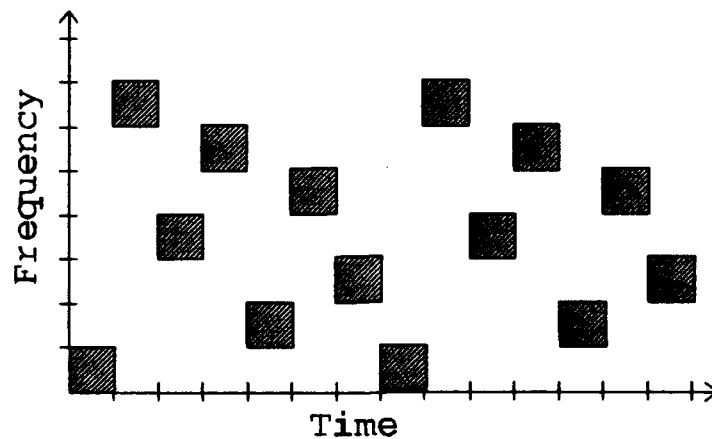


**Figure 2.4: Frequency Hopping Spread Spectrum**

Figure 2.5 is an illustration of a basic frequency-hopped transmitter. The clock controls the FSR at the hop rate which may or not be faster than the data rate. This thesis concentrates on systems where the hop rate is from one to four times the data rate. The FSR in Figure 2.5 has three registers which have seven different states that are sent to a digital-to-analog converter (DAC). The DAC takes the seven

different digital symbols and converts them to seven different voltage levels. These voltage levels are then sent to a voltage-controlled oscillator (VCO) which converts the seven different voltage levels to seven different frequencies. These frequencies hop through the seven different values according to the pattern that is dictated by the FSR. Now the output of the VCO and the mixer act like a simple carrier modulator where the carrier frequency follows the hop pattern and modulates the data to one of the seven different carrier frequencies.

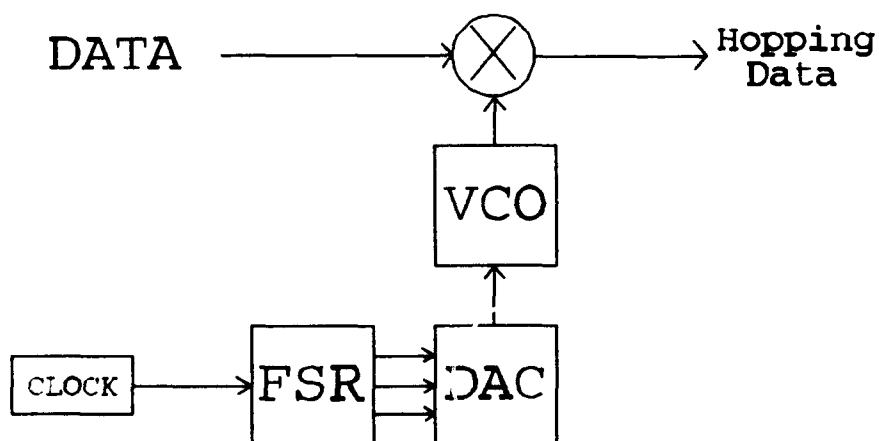


**Figure 2.5: Frequency Hopping Transmitter**

Figure 2.6 is an illustration of basic frequency-hopped receiver. The radio-frequency amplifier (RF AMP) simply amplifies the received signal for processing. Before the signal can be dehopped, the receiver must synchronize to the incoming signal. This is done by setting up a trap filter that only passes one of the hop frequencies in the channel. When the incoming signal is at this hop frequency, the trap filter passes the signal to the envelope detector which in turn passes a voltage to the threshold detector. When the incoming signal is at the trap filter's frequency, the threshold detector receives a voltage higher than its threshold and sends a voltage to the FSR to reset to this frequency. Then the right half of the loop begins to step through the hopping pattern beginning at the synchronization frequency and is correctly synchronized with the incoming signal. When this occurs, the output of the mixer is the sum and difference frequencies of the two inputs to the mixer. If the two inputs are synchronized, as they should be, the difference frequencies will remain fixed from hop to hop. A simple low-pass filter will remove the sum frequencies. If a signal is received at the trap frequency that is not properly coded, the receiver will receive garbage. When a properly coded signal is received, the receiver synchronizes to it and remains synchronized.



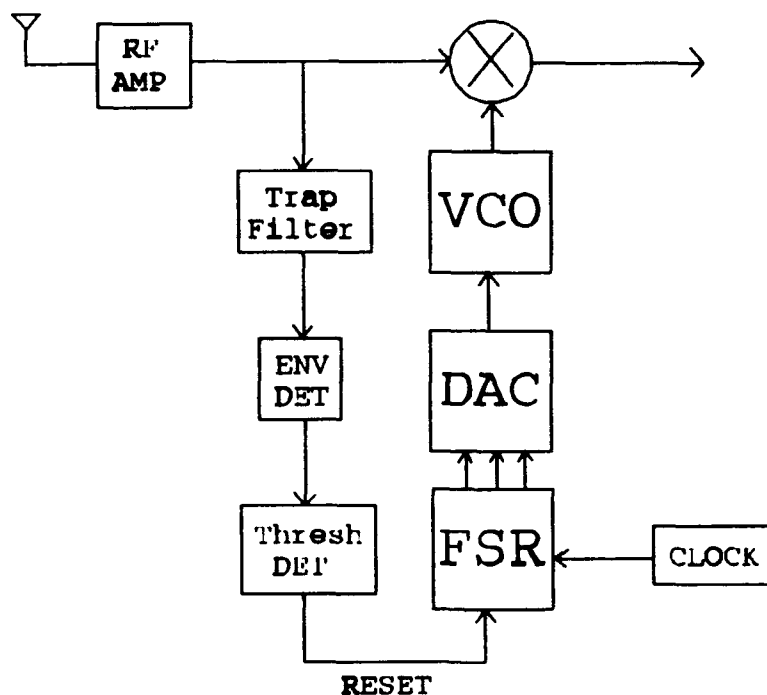


**Figure 2.6: Frequency Hopping Receiver**

The difference between frequency-hopped spread spectrum and direct sequence spectrum is that the signal itself is not encrypted, and cannot be buried in noise to be covert. However, frequency-hopped spread spectrum provides some immunity from multipath errors that result from signals arriving after the information has changed and gives immunity to jamming and interference as this thesis shows.

Fast-Frequency hopping implies that the hopping rate is greater than the data rate so that a bit of data is transmitted multiple times at several different carrier frequencies. For example, if the hopping rate is three times

as fast as the data rate, then the circuit is said to have a diversity ( $L$ ) of three. This means that three successive hops will carry the same information and if one of these hops is jammed, the other hops will provide redundancy.

One problem with fast frequency hopping is that diversity results in losses when the information is recombined in the receiver. This is known as non-linear combining losses [REF 3]. To understand this, think of the result of trying to cut a paper into four pieces and then gluing them back together again. It is impossible to get the same paper back again.

In this thesis, one of the considerations that must be explored is at what point do the non-linear combining losses overcome the gains due to diversity for the ratio-statistic combining receiver. The affect of nonlinear combining losses and fading remain the same over the range of jamming. As the signal-to-jammer ratio becomes large, the affect of nonlinear combining losses become apparent. If the amount of fading is low, nonlinear combining losses dominate and diversity becomes a disadvantage. Later in the thesis this will be shown.

#### **B. FREQUENCY SHIFT KEYING (FSK)**

The modulation technique used in this thesis is frequency-shift keying (FSK). FSK is a modulation technique where each symbol is represented by a different frequency carrier. Figure 2.7 is an example of  $M$ -ary FSK where  $M$  equals four.  $M$  represents the number of different frequencies used to

modulate the data. Each frequency represents a symbol in the symbol alphabet. The information in this case is in frequency two which may represent the symbol 01. The other three frequencies contain nothing but thermal noise. If  $M$  is equal to two, the signal is Binary FSK (BFSK) and there are two frequencies representing either '1' or '0'.

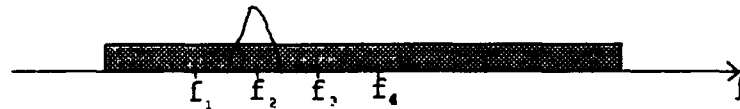


**Figure 2.7: M-ARY FSK**

Figure 2.8 is an illustration of a typical BFSK receiver. For each carrier frequency, there is a corresponding branch in the receiver with a band-pass filter designed for that frequency. Ideally, the branch with the highest voltage out of the filter is the branch which contains the signal. In the figure, the upper branch represents a logical '0', and the lower branch represents a logical '1'. In a clear channel with no interference, if a '0' is transmitted, the output of the upper branch is significantly higher than the output of

the lower branch and the decision statistic ( $w$ ) is positive. The probability of error is the probability that  $w$  is negative. Note that the signal must be dehopped before the FSK demodulator can be applied. A noncoherent receiver implies that the receiver has no knowledge of the phase or amplitude of the received signal.

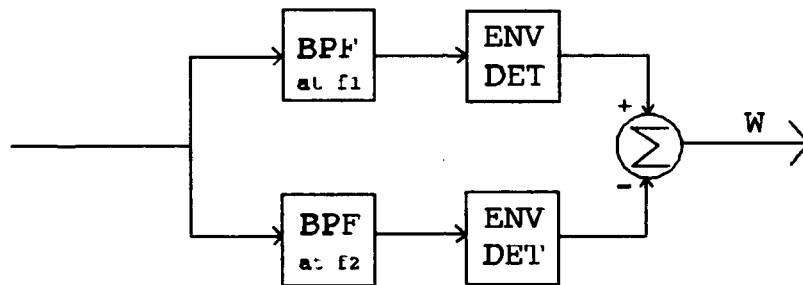


**Figure 2.8: BFSK Receiver**

In this thesis, the binary case is examined for a square-law detector and an envelope detector. Then the system is modified to include the  $M$ -ary case.

## 1. Envelope Detector

Figure 2.9 shows the basic operation of an envelope detector. In the figure, the original information is a sine wave. This information is modulated up to a much higher frequency. The envelope detector simply follows the peaks of the received signal to trace out the original sine wave [REF 4 and 5]. Note that the sine wave has a DC component to make it all positive. Otherwise, the envelope detector output is a rectified sine wave. Assuming that the sine wave has a DC component that causes the original signal to be positive at all points, as can be seen in the example of Figure 2.9, we see that the envelope of the received signal is the original signal.

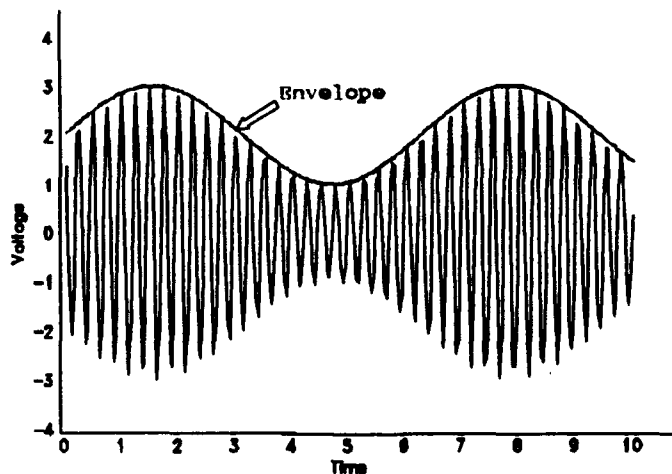


**Figure 2.9: Envelope Detection Of A Sine Wave**

## **2. Square-Law Detector**

The square-law detector demodulates the signal by first squaring it and then passing it through a low pass filter to remove the DC component [REF 4 and 5]. The square-law detector is effectively an envelope detector squared. Both the envelope detector and the square-law detector serve well as noncoherent receivers.

### **C. Partial-Band Jamming**

Since the system uses frequency-hopping spread spectrum techniques to modulate the data, it is reasonable to assume that a hostile jammer will be unable to jam the entire frequency band of the system. It is not reasonable to assume, however, that the jammer will not jam a portion of the band. It may be possible to jam enough of the band that the probability of bit error in the receiver will be too high to use the data. Also, the jammer can hop around in a pseudo random fashion known only to him to prevent the receiver from simply deemphasizing the jammed portion of the frequency band.

This practice of jamming a portion of the band is known as partial-band jamming. The portion of the signal that does not fall within the jammed portion of the frequency band is unaffected by the jamming, but every hop which falls in the jammed region has a higher probability of bit error and must be considered. Figure 2.10 is an illustration of a band that has partial-band jamming.

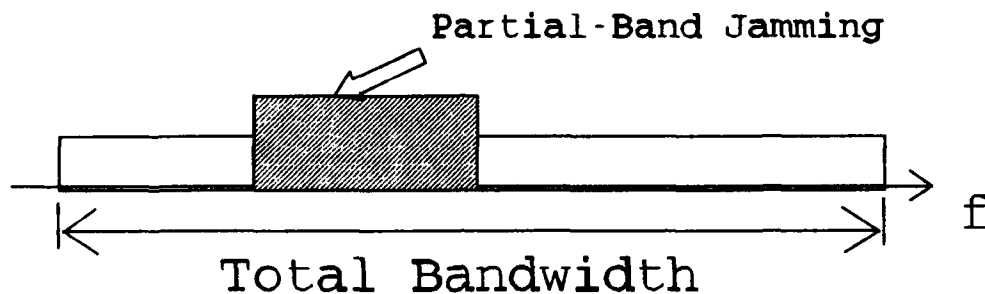


**Figure 2.10: Partial-Band Jamming**

There are two parameters that the jammer has to choose. It must choose the amount of the band to jam ( $\gamma$ ) and the amount of power to jam with in order to achieve a desired signal-to-jammer ratio over this band. In Figure 2.10, these two parameters represent the width and the height of the jamming respectively. In this thesis, several values of  $\gamma$  will be examined over a wide range of signal-to-jammer ratios.

#### **D. Rician Fading**

In this thesis, a channel with Rician fading is assumed. Fading is what happens to a signal as it travels through the channel. The signal can bounce off buildings, mountains, etc.

or be attenuated in the atmosphere. The result is that some portion of the signal reaches the receiver by a direct channel and another portion reaches the receiver by a diffuse (or indirect) channel.

Figure 2.11 is an illustration of a system involving a geosynchronous satellite and a fixed ground station with a highly directional antenna. In this case the only signal that reaches the receiver is by the direct (line-of-sight) path. This channel has no fading.

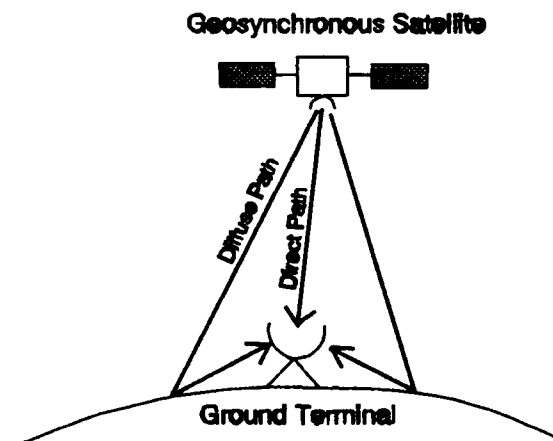


**Figure 2.11: Geosynchronous Satellite to Fixed Ground Terminal Link.**



Figure 2.12 is an illustration of a system involving two mobile ground stations with omni-directional antennas where the line-of-sight is obstructed. In this case, no signal reaches the receiver by the direct path. All the signal reaches the receiver by the diffuse path and this channel has Rayleigh fading.

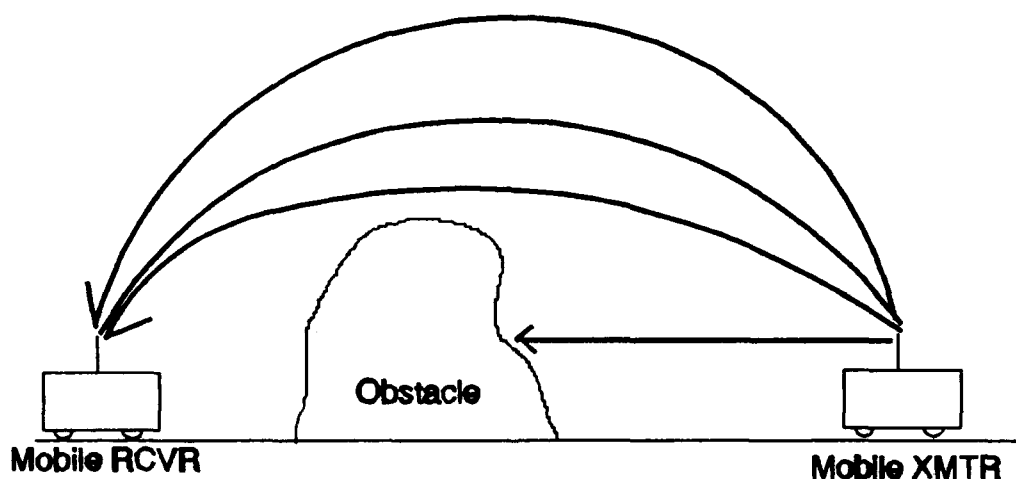


**Figure 2.12: Mobile-To-Mobile Ground Link**

Figure 2.13 is an illustration of a system involving a low altitude satellite and a mobile ground station with an omni-directional antenna. In this case, the signal reaches the receiver by both the direct and diffuse path. This channel

has Rician fading. The ratio of direct-to-diffuse power is an important parameter that is discussed later.

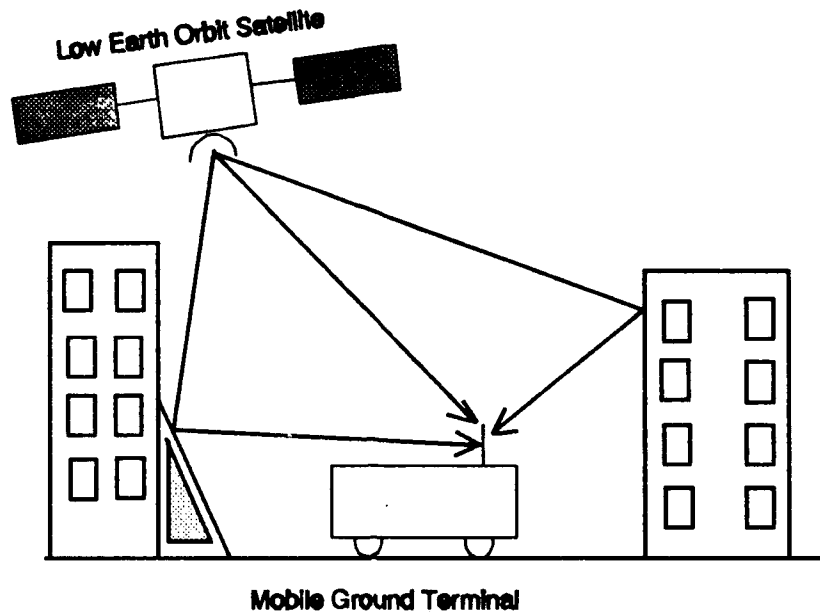


**Figure 2.13: Low Earth Orbit to Mobile Ground Terminal Link.**

The best way to understand Rician fading is to think of a bull's eye dart board. The dart is thrown at the dart board and sticks at some distance from the bull's eye. The  $X$  or  $Y$  coordinate of the distance from the bull's eye will obey a Gaussian probability distribution. The distance from the bull's eye to the dart obeys a Rayleigh probability distribution. Therefore, the Rayleigh random variable  $D$ , which represents the distance from the bull's eye to the dart,

is related to the Gaussian random variables  $X$  and  $Y$  by Equation (1). A Rician random variable is the same as a Rayleigh random variable except that the origin is not assumed to be at the point  $(0,0)$  [REF 6].

$$D = \sqrt{X^2 + Y^2} \quad (1)$$

#### E. RATIO-STATISTIC COMBINING

The main focus of this thesis is to examine the performance of a fast frequency-hopped  $M$ -ary FSK system with ratio-statistic combining in the presence of partial-band jamming and Rician fading. The name, ratio-statistic, implies that the decision statistic for the circuit is a ratio. Figure 2.14 is an illustration of a basic ratio-statistic combiner for a BFSK receiver after the signal has been dehopped [REF 2]. As illustrated in Figure 2.14, the BFSK signal is first demodulated as in Figure 2.8. Then the voltages ( $x_{11}$  and  $x_{21}$ ) at the output of the envelope detectors (or square-law detectors) are compared to determine which is the largest. The largest voltage is inverted and multiplied with each of the two original voltages. The result is the variables  $t_{11}$  or  $t_{21}$  as illustrated in Figure 2.14. The effect of the ratio-statistic operation, which divides each branch of the receiver by the greater of the two, is that one branch will now have a voltage of one and the other will have a voltage less than one. If the jammer uses a large amount of

power to jam a narrow band so that a jammed hop will have a very large voltage level, the ratio-statistic combiner limits the maximum output to one volt. The next step in the process is to sum up all the hops that make up the current data bit. If the diversity of the signal is three, then three hops are summed to comprise the overall decision statistic. If one of the three hops is in error, then the other two can compensate since the hop in error can only be one volt in the wrong direction. In other words, hops that are strongly affected by jamming, leading to large values of  $x_{11}$  and  $x_{21}$ , will not dominate  $w_1$  as in a conventional BFSK receiver with fast frequency-hopping. For example, if a logical '0' is transmitted with a diversity of three, then in the ideal case  $w_1$  is equal to three while  $w_2$  equals zero. If one of the hops is in error, then, for that hop,  $t_{21}$  would equal one and  $t_{11}$  is less than one but greater than zero. However,  $w_1$  is still greater than  $w_2$ ,  $R$  is still positive, and the original data bit is correctly determined. As long as the jamming is across a narrow band, diversity and the ratio-statistic combiner should be able to counteract some of the effects of the jammer. The degree of this counteraction is the focus of this thesis.

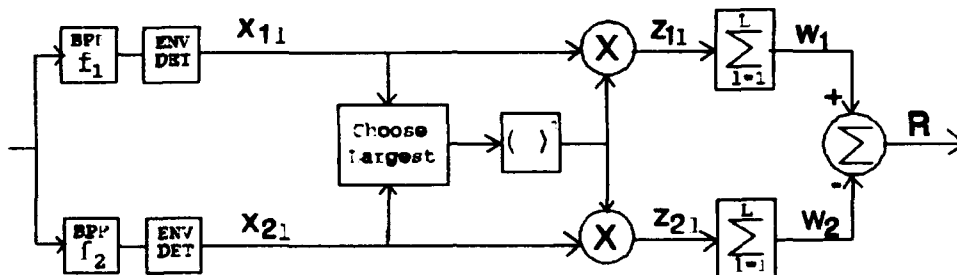


**Figure 2.14: Block Diagram for a Receiver Employing Ratio-Statistic Combining.**

### III. MATHEMATICAL ANALYSIS

#### A. INITIAL GOALS OF DERIVATION

Figure 3.1 is an illustration of an alternate way of implementing the receiver shown in Figure 2.14. Since the summation operations are linear operations, their order can be interchanged with the result that the analytical portion of the performance analysis can go farther than otherwise. In Figure 3.1, the random variables  $x_{11}$  and  $x_{21}$  are both normalized to form the random variables  $z_{11}$  and  $z_{21}$ , where

$$z_{11} = \frac{x_{11}}{q_1} \quad (3)$$

where  $i=1$  or  $2$ , and

$$q_i = \max(x_{1i}, x_{2i}) \quad (4)$$

Since  $z_{11}$  and  $z_{21}$  both vary between 0 and 1, it can be seen that the random variable  $y_1$  varies from -1 to +1, and the random variable  $w$  varies from  $-L$  to  $+L$ . When a signal at frequency  $f_1$  is transmitted, an error occurs when  $w$  is negative. Therefore, the goal of the analysis is to find the probability density function for  $f_w(w)$ . The probability of bit error is

$$P_{be} = \int_{-L}^0 f_v(w) dw \quad (5)$$

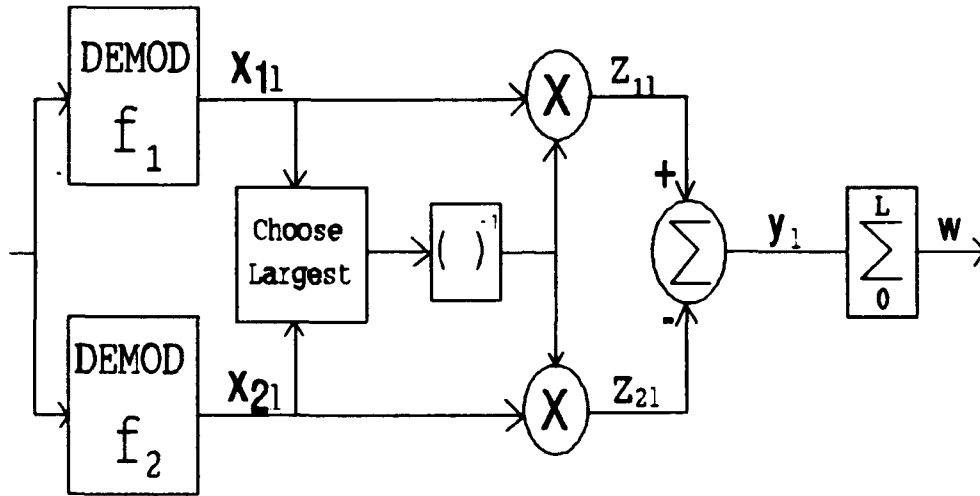


**Figure 3.1. Alternate Implementation of the Ratio-Statistic Receiver.**

The probability of bit error ( $P_{be}$ ) for a diversity ( $L$ ) and jamming duty factor ( $\gamma$ ) is

$$P_{be} = \sum_{j=0}^L \binom{L}{j} \gamma^j (1 - \gamma)^{L-j} P(e; j) \quad (6)$$

where  $P(e; j)$  is the conditional probability of error given  $j$  of  $L$  hops are jammed. If the hop is jammed, it has a higher probability of bit error than if it is not. The number of

hops that are jammed will depend on the duty factor of the jamming ( $\gamma$ ). By summing over all possible values of  $j$ , the total probability of bit error is found. All that remains is to determine  $P(e; j)$ .

There are two different sets of pdf's for  $y_1$  and  $w$ : one for the case when interference is not present and one for the case when interference is present. The difference does not effect the derivation of  $f_{y_1}(y_1)$ . Only the signal-to-noise ratio will be different.

The interference is modeled as additive white Gaussian noise which is present in both the detectors of the FSK demodulator with a probability equal to the duty factor of the interference.  $N_j/2$  is the power spectral density of the jammer.  $N_o/2$  is the power spectral density of thermal noise. The total noise power spectral density when interference is present is

$$\frac{N_T}{2} = \frac{N_o}{2} + \frac{N_j}{2\gamma} \quad (7)$$

The noise power at the receiver when no interference is present is

$$\sigma_1^2 = N_o B \quad (8)$$

with a probability of  $\gamma$  where  $B$  is the equivalent noise bandwidth of the bandpass filters in both branches of the FSK



receiver. The noise power at the receiver when interference is present is

$$\sigma_k^2 = (\gamma^{-1}N_j + N_o) B \quad (9)$$

with a probability of  $1-\gamma$ .

The bit rate is defined as  $R_b = 1/T_b$  where the duration of a bit interval is taken to be  $T_b$  seconds. The duration of hop interval, for a diversity of  $L$  hops per bit, is  $T_h = T_b/L$  and the hop rate is  $R_h = 1/T_h = LR_b$ . The average energy per hop is  $E_h = ST_h$  where  $S$  is the average signal power. The average energy per bit is  $E_b = LE_h$ . The signal power-to-noise power ratio is

$$\frac{S}{\sigma_1^2} = \frac{E_h R_h}{N_r B} = \frac{E_b R_b}{LN_r B} \quad (10)$$

The equivalent noise bandwidth of the filter is taken to equal to the hop rate, that is  $B = R_h$  is chosen and

$$\frac{S}{\sigma_1^2} = \frac{E_b}{LN_r} \quad (11)$$

The analytical derivation is carried out for the probability density function (pdf) for the random variable  $w$ . The derivation of the pdf for  $w$  requires  $L$  convolutions.

analytical solution for  $f_w(w)$  has not been found and is done numerically.

The first step is to derive the pdf at the demodulator output for each of the branches ( $x_{11}$  and  $x_{21}$ ). The second step is to derive the pdf of  $y_1$ .

The dehopped signal is expressed as

$$s(t) = \sqrt{2} a \cos(\omega t + \theta), 0 \leq t \leq T_b \quad (12)$$

where  $\omega$  is the frequency of the signal,  $\theta$  is the phase of the signal, and  $\sqrt{2} a$  is the signal amplitude. The amplitudes of all hops are assumed to be the same, that is  $a_1 = a_2 = \dots = a_1$ . Hence, the average signal power is

$$\overline{s^2} = \frac{1}{2} \overline{(\sqrt{2} a)^2} = \overline{a^2} \quad (14)$$

#### B. BFSK ENVELOPE DETECTOR

If the signal is assumed to be present in the upper branch of the receiver, then

$$f_{x_{11}}(x_{11} | a) = \frac{x_{11}}{\sigma_1^2} e^{-\frac{(x_{11}^2 + 2a^2)}{2\sigma_1^2}} I_0\left(\frac{\sqrt{2} a x_{11}}{\sigma_1^2}\right) \quad (15)$$

which is conditional on  $a$  being present. Since the lower branch has no signal present,  $a = 0$  and this Rician density function reduces to the Rayleigh density function

$$f_{x_{21}}(x_{21}) = \frac{x_{21}}{\sigma_1^2} e^{-\frac{x_{21}^2}{2\sigma_1^2}} \quad (16)$$

which is not conditional on  $a$ . There is no fading if  $a$  is not a random variable.

### 1. Forming the Joint Density Function

Since  $x_{11}$  and  $x_{21}$  are independent random variables, the joint density function of the two random variables is obtained by the product of the two pdf's as [REF 6]

$$f_{x_{11}x_{21}}(x_{11}x_{21}|a) = \frac{x_{11}x_{21}}{\sigma_1^4} e^{-\frac{(x_{11}^2 + x_{21}^2 + 2a^2)}{2\sigma_1^2}} I_0\left(\frac{\sqrt{2}ax_{11}}{\sigma_1^2}\right) \quad (17)$$

### 2. Setting Up The Auxiliary Variable

In order to obtain  $f_{y_1}(y_1)$ , the method of auxiliary variables is used [REF 7].

There are two cases from this point on. The first case is when  $x_{21}$  is greater than  $x_{11}$ , and the second case is when  $x_{11}$  is greater than  $x_{21}$ . For the first case, it can be seen that the random variable  $y_1$  falls between  $-1$  and  $0$ . For the second

case,  $y_1$  falls between 0 and 1. These two cases have separate derivations which will be handled in parallel.

The auxiliary variables are chosen as follows for  $-1 \leq y_1 < 0$

$$y_1 = \frac{x_{11} - x_{21}}{x_{21}} \quad (18)$$

If one defines

$$x_{21} = u \quad (19)$$

then

$$x_{11} = u(1 + y_1) \quad (20)$$

and for  $0 \leq y_1 \leq 1$ :

$$y_1 = \frac{x_{11} - x_{21}}{x_{11}} \quad (21)$$

and defining

$$x_{11} = u \quad (22)$$

one obtains

$$x_{21} = u(1 - y_1) \quad (23)$$

### 3. The Joint Density Theorem

In order to obtain  $f_{y_1 u}(y_1 u)$ , the joint density theorem is used [REF 7]. This theorem is as follows:

To find  $f_{zw}(zw)$ , solve the system

$$z = g(x, y) \quad w = h(x, y) \quad (24)$$

where

$$f_{zw}(zw) = \frac{f_{xy}(x_1, y_1)}{|J(x_1, y_1)|} + \dots + \frac{f_{xy}(x_n, y_n)}{|J(x_n, y_n)|}, \dots \quad (25)$$

and

$$J(x, y) = \begin{vmatrix} \frac{\partial z}{\partial x} & \frac{\partial z}{\partial y} \\ \frac{\partial w}{\partial x} & \frac{\partial w}{\partial y} \end{vmatrix} \quad (26)$$

is the Jacobian of the transformation.

Since  $y_1$  and  $u$  are known as a function of  $x_{11}$  and  $x_{21}$ , then the transformation can be accomplished by dividing  $f_{x_{11}, x_{21}}(x_{11}, x_{21})$  by the absolute value of the Jacobian as in Equation (24). The Jacobians for each of the two cases are

$$J = \frac{1}{x_{21}} = \frac{1}{u}, \quad -1 \leq y_1 \leq 0 \quad (27)$$

and

$$J = \frac{1}{x_{11}} = \frac{1}{u}, \quad 0 \leq y_1 \leq 1 \quad (28)$$

With these Jacobians, the auxiliary variables of Equations (17)-(22), and Equation (16), the joint density function of  $y_1$  and  $u$  are

$$f_{y_1 u}(y_1 u | a) = u f_{x_{11} x_{21}}[u(1+y_1), u | a], \quad -1 \leq y_1 \leq 0 \quad (29)$$

which yields

$$f_{y_1 u}(y_1 u | a) = \frac{u^3 (1+y_1)}{\sigma_1^4} e^{-\frac{(u^2(1+y_1)^2 + u^2 + 2a^2)}{2\sigma_1^2}} I_0\left(\frac{\sqrt{2} a u (1+y_1)}{\sigma_1^2}\right), \quad -1 \leq y_1 \leq 0 \quad (30)$$

and

$$f_{y_1 u}(y_1 u | a) = u f_{x_{11} x_{21}}[u, u(1-y_1) | a], \quad 0 \leq y_1 \leq 1 \quad (31)$$

which yields

$$f_{y_1 u}(y_1 u | a) = \frac{u^3 (1-y_1)}{\sigma_1^4} e^{-\frac{(u^2(1-y_1)^2 + u^2 + 2a^2)}{2\sigma_1^2}} I_0\left(\frac{\sqrt{2} a u}{\sigma_1^2}\right), \quad 0 \leq y_1 \leq 1 \quad (32)$$

#### 4. Integrating Out The Auxiliary Variable

Now that the joint density functions for  $u$  and  $y_1$  have been determined, the next step is to integrate Equations (29) and (31) over  $u$  from 0 to  $\infty$  to obtain  $f_{y_1}(y_1)$ . Using the identity [REF 10]

$$\int_0^{\infty} x^{n+\frac{v}{2}} e^{-ax} J_v[2\beta\sqrt{x}] dx = n! \beta^v e^{-\frac{\beta^2}{a}} a^{-(n+v-1)} L_n^v\left(\frac{\beta^2}{a}\right), \quad n+v > -1 \quad (33)$$

One obtains the final results conditional on  $a$  as follows:

$$f_{y_1}(y_1|a) = \frac{2(1+y_1)}{[1+(1+y_1)^2]^2} e^{-\frac{a^2}{\sigma_1^2[1+(1+y_1)^2]}} \left[ 1 + \frac{a^2(1+y_1)^2}{\sigma_1^2[1+(1+y_1)^2]} \right], \quad -1 \leq y_1 \leq 0 \quad (34)$$

and

$$f_{y_1}(y_1|a) = \frac{2(1-y_1)}{[1+(1-y_1)^2]^2} e^{-\frac{a^2}{\sigma_1^2[1+(1-y_1)^2]}} \left[ 1 + \frac{a^2}{\sigma_1^2[1+(1-y_1)^2]} \right], \quad 0 \leq y_1 \leq 1 \quad (35)$$

#### 5. Adding Rician Fading

In order to take fading in the channel into account, the signal amplitude is assumed to be a Rician random variable

$$f_a(a) = \frac{a}{\sigma^2} e^{-\frac{(a^2 + \alpha^2)}{2\sigma^2}} I_0\left(\frac{a\alpha}{\sigma^2}\right) \quad (36)$$

where  $\alpha^2$  is the average signal power in the direct component of the signal and  $2\sigma^2$  is the average signal power in the diffuse component of the signal.

Now the unconditional pdf for  $y_1$  is

$$f_{y_1}(y_1) = \int_0^{\infty} f_{y_1}(y_1|a) f_a(a) da \quad (37)$$

## 6. Final Probability Density Functions

After integrating out the Rician fading, two substitutions were made to simplify the understanding of the final density functions.

The diffuse signal-to-noise ratio is defined as

$$\xi_1 = \frac{2\sigma^2}{\sigma_1^2} \quad (38)$$

and the direct signal-to-noise ratio is defined as

$$\rho_1 = \frac{\alpha^2}{\sigma_1^2} \quad (39)$$



With these definitions, Equation (36) is evaluated to obtain

$$f_{y_1}(y_1) = \frac{2(1+y_1)}{[1+(1+y_1)^2][1+\xi_1+(1+y_1)^2]} e^{-\frac{\rho_1}{1+\xi_1+(1+y_1)^2}} \quad (40)$$

$$\times \left[ 1 + \frac{(1+y_1)^2}{1+\xi_1+(1+y_1)^2} \left( \xi_1 + \frac{\rho_1(1+(1+y_1)^2)}{1+\xi_1+(1+y)^2} \right) \right], \quad -1 \leq y_1 \leq 0$$

and

$$f_{y_1}(y_1) = \frac{2(1-y_1)}{[1+(1-y_1)^2][1+(\xi_1+1)(1-y_1)^2]} e^{-\frac{\rho_1(1-y_1)^2}{1+(\xi_1+1)(1-y_1)^2}}$$

$$\times \left[ 1 + \frac{1}{1+(\xi_1+1)(1-y_1)^2} \left( \xi_1 + \frac{\rho_1(1+(1-y_1)^2)}{1+(\xi_1+1)(1-y_1)^2} \right) \right], \quad 0 \leq y_1 \leq 1 \quad (41)$$

### C. BFSK SQUARE-LAW DETECTOR

The procedure for deriving  $f_{y_1}(y_1)$  for a BFSK square-law detector is the same as for a BFSK envelope detector. Figure

3.1 still applies except that the demodulators use square-law detectors instead of envelope detectors.

If the signal is assumed to be present in the upper branch of the receiver, then

$$f_{x_{1l}|a}(x_{1l}|a) = \frac{1}{2\sigma_1^2} e^{-\frac{(x_{1l} + 2a^2)}{2\sigma_1^2}} I_0\left(\frac{a\sqrt{2x_{1l}}}{\sigma_1^2}\right) \quad (42)$$

and

$$f_{x_{2l}}(x_{2l}) = \frac{1}{2\sigma_1^2} e^{-\frac{x_{2l}}{2\sigma_1^2}} \quad (43)$$

### 1. Forming the Joint Density Function

As with the envelope detector, the joint density function is the product of Equations (41) and (42) which yields

$$f_{x_{1l}x_{2l}|a}(x_{1l}x_{2l}|a) = \frac{1}{4\sigma_1^4} e^{-\frac{(x_{1l} + x_{2l} + 2a^2)}{2\sigma_1^2}} I_0\left(\frac{a}{\sigma_1^2}\sqrt{2x_{1l}}\right) \quad (44)$$

## 2. Finding $f_{y_1}(y_1)$

The auxiliary variables for the square-law detector are the same as with the envelope detector and given by Equations (17)-(22). The joint density theorem is applied again as described in Section III.B.3. The Jacobians also are given by Equation (26) and (27). The joint density functions of  $y_1$  and  $u$  and the result of integrating out the auxiliary variable  $u$  for each case are

$$f_{y_1 u}(y_1 u | a) = u f_{x_1 x_2} [u(1+y_1), u | a], -1 \leq y_1 \leq 0 \quad (45)$$

which becomes

$$f_{y_1 u}(y_1 u | a) = \frac{1}{4\sigma_1^4} e^{-\frac{(u(1+y_1) + u + 2a^2)}{2\sigma_1^2}} I_0\left(\frac{a}{\sigma_1^2} \sqrt{2u(1+y_1)}\right), -1 \leq y_1 \leq 0 \quad (46)$$

with the final result

$$f_{y_1}(y_1 | a) = \frac{1}{(2+y_1)^2} e^{-\frac{a^2}{\sigma_1^2(2+y_1)}} \left[ 1 + \frac{a^2(1+y_1)}{\sigma_1^2(2+y_1)} \right], -1 \leq y_1 \leq 0 \quad (47)$$

and

$$f_{y_1 u}(y_1 u | a) = u f_{x_1 x_2} [u, u(1-y_1) | a], 0 \leq y_1 \leq 1 \quad (48)$$

which becomes

$$f_{y_1 u}(y_1 u | a) = \frac{1}{4\sigma_1^4} e^{-\frac{(u(1-y_1) + u + 2a^2)}{2\sigma_1^2}} I_0\left(\frac{a}{\sigma_1^2} \sqrt{2u}\right), 0 \leq y_1 \leq 1 \quad (49)$$

with the final result

$$f_{y_1}(y_1 | a) = \frac{1}{(2-y_1)^2} e^{-\frac{a^2(1-y_1)}{\sigma_1^2(2-y_1)}} \left[ 1 + \frac{a^2}{\sigma_1^2(2-y_1)} \right], 0 \leq y_1 \leq 1 \quad (50)$$

### 3. Final Probability Density Functions

Fading is taken into account in the same manner as in Section III.B.5. Equation (35) is the pdf of the Rician fading. The products of Equation (46) or (49) and Equation (35) are integrated over  $a$  as shown in Equation (36) to obtain the density function as follows:

$$f_{y_1}(y_1 | a) = \frac{1}{(2+y_1)(2+\xi_1+y_1)} e^{-\frac{\rho_1}{2+\xi_1+y_1}} \times \left[ 1 + \frac{(1+y_1)}{2+\xi_1+y_1} \left( \xi_1 + \frac{\rho_1(2+y_1)}{2+\xi_1+y_1} \right) \right], -1 \leq y_1 \leq 0 \quad (51)$$

and

$$f_{y_1}(y_1) = \frac{1}{(2-y_1) [2-y_1+\xi_1(1-y_1)]} e^{-\frac{\rho_1(1-y_1)}{2-y_1+\xi_1(1-y_1)}} \quad (52)$$

$$\times \left[ 1 + \frac{1}{2-y_1+\xi_1(1-y_1)} \left( \xi_1 + \frac{\rho_1(2-y_1)}{2-y_1+\xi_1(1-y_1)} \right) \right], 0 \leq y_1 \leq 1$$

where  $\xi_1$  and  $\rho_1$  are defined in Equations (37) and (38), respectively.

#### D. Special Case For $L=1$

For the special case when  $L=1$ , it is possible to evaluate the probability of bit error analytically. Since for  $L = 1$ ,

$$f_{y_1}(y_1) = f_w(w) \quad (53)$$

then Equation (52) can be substituted into Equation (4) to yield

$$P_{be} = \int_{-1}^0 f_{y_1}(y_1) dy_1 \quad (54)$$

By substituting Equations (39) and (50) into Equation (53), the probability of bit error is obtained for the envelope detector and the square-law detector, respectively.

### 1. Envelope Detector

The first step is to make a simple change of variables with

$$v = \frac{1}{1 + \xi_1 + (1 + y_1)^2} \quad (55)$$

Therefore

$$dv = \frac{-(2 + 2y_1) dy_1}{[1 + \xi_1 + (1 + y_1)^2]^2} = -v^2 (2 + 2y_1) dy_1 \quad (56)$$

and

$$y_1 = \sqrt{\frac{1 - (1 + \xi_1) v}{v}} - 1 \quad (57)$$

and

$$dy_1 = \frac{-dv\sqrt{v}}{2v^2\sqrt{1 - (1 + \gamma_1) v}} \quad (58)$$

Substituting Equation (55) into Equation (39), one gets

$$f_{y_1}(v) = e^{-v p_1} \left[ \frac{2v^2 \sqrt{\frac{1-(1+\gamma_1)v}{v}}}{(1-\gamma_1 v)} \right] \quad (59)$$

$$\times [1 + [1 - (1+\gamma_1)v] (\gamma_1 + p_1(1-\gamma_1 v))] ]$$

Substituting Equation (58) into

$$P_{be} = \int_{\frac{1}{1+\xi_1}}^{\frac{1}{2+\xi_1}} f_{y_1}(v) \left[ \frac{-dv\sqrt{v}}{2v^2 \sqrt{1-(1+\gamma_1)v}} \right] \quad (60)$$

where the limits of the integral are transformed to reflect  $v$  when  $y_1 = -1$  to  $0$ , one gets

$$f_{y_1}(v) = - \int_{\frac{1}{2+\gamma_1}}^{\frac{1}{1+\gamma_1}} e^{-v p_1} \left( \frac{1}{1-\gamma_1 v} \right) [1 + (1-v-\gamma_1 v) (\gamma_1 + p_1 - \gamma_1 p_1 v)] dv \quad (61)$$

which reduces to

$$f_{y_1}(v) = - \int_{\frac{1}{2+y_1}}^{\frac{1}{1+y_1}} e^{-vp} (1 + \gamma_1 + \rho_1 - v\rho_1 - v\rho_1\gamma_1) dv \quad (62)$$

The result of the integration is the simple equation

$$P_{be} = \frac{e^{\frac{-\rho_1}{2+\xi_1}}}{2+\xi_1} \quad (63)$$

## 2. Square Law Detector

The procedure for the square-law detector is the same as for the envelope detector. The first step is to make a simple change of variables with

$$v = \frac{1}{\xi_1 + 2 + y_1} \quad (64)$$

and

$$dv = \frac{-dy_1}{(\xi_1 + 2 + y_1)^2} = -v^2 dy_1 \quad (65)$$

Therefore



$$y_1 = \frac{1-v(2+\xi_1)}{v} \quad (66)$$

Substituting Equation (65) into Equation (50), one gets

$$\begin{aligned} f_{y_1}(v) = & -\frac{e^{-v\rho_1}}{v^2} \left( \frac{v}{2 + \frac{1-v(2+\xi_1)}{v}} \right) \\ & \times \left[ 1 + v \left( 1 + \frac{1-v(2+\xi_1)}{v} \right) \left( \xi_1 + v\rho_1 \left( 2 + \frac{1-v(2+\xi_1)}{v} \right) \right) \right] \end{aligned} \quad (67)$$

which reduces to

$$\begin{aligned} f_{y_1} = & v^2 e^{-\rho_1 v} \left( \frac{1}{1-v\xi_1} \right) \times \\ & [1 + \xi_1 - v\xi_1 - \xi_1^2 v + \rho_1 - v\rho_1 - \xi_1 v\rho_1 - v\xi_1 \rho_1 + v^2 \xi_1 \rho_1 + \xi_1^2 v^2 \rho_1] \end{aligned} \quad (68)$$

Now

$$P_{be} = \int_{\frac{1}{1+\xi_1}}^{\frac{1}{2+\xi_1}} f_{y_1}(v) \left[ \frac{-dv}{v^2} \right] \quad (69)$$

Where the limits of the integral are transformed to reflect  $v$  when  $y_1 = -1$  to  $0$ . The result of the integration is the simple equation

$$P_{be} = \frac{e^{\frac{-p_1}{2+\xi_1}}}{2+\xi_1} \quad (70)$$

which is identical to Equation (62). This shows that, for a diversity of one, the envelope detector and the square-law detector have identical performance.

#### E. M-ARY FSK DERIVATION

The next step is to extend the derivation to the  $M$ -ary case. Figure 3.2 is an illustration of an  $M$ -ary FSK receiver with ratio-statistic combining. The ratio-statistic combiner selects the largest voltage of all the branches for each hop and then divides each branch by this voltage so that one branch is normalized to one volt and the rest are between zero and one.

Hence

$$z_{1i} = \frac{x_{1i}}{q_1} \quad (71)$$

where  $i = 1, 2, 3, \dots, M$  and

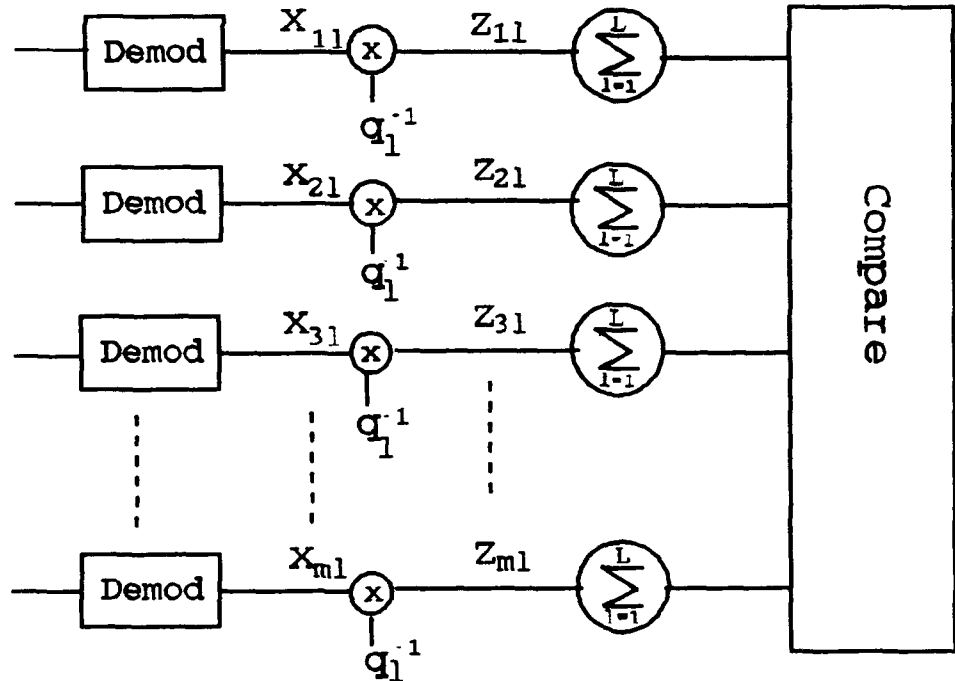


Figure 3.2: M-ary FSK Receiver

$$q_1 = \max(x_{11}, x_{21}, x_{31}, \dots, x_{M1}) \quad (72)$$

The overall decision statistics for each branch are obtained by summing over all hops of a symbol

$$Z_i = \sum_{l=1}^L Z_{il} \quad (73)$$

where  $i = 1, 2, 3, \dots, M$ .

The derivation assumes that the signal is present in branch one. The probability of symbol error is

$$P_s = \Pr(z_1 < z_2 \cup z_1 < z_3 \cup \dots \cup z_1 < z_M) \quad (74)$$

### 1. Union Bound

The random variables  $z_1$  are not statistically independent. As a result, a union bound is used to give a worst case solution for the probability of bit error.

For two random variables

$$P(A \cup B) = P(A) + P(B) - P(A \cap B) \quad (75)$$

In this case, the third term represents the intersection of the probabilities of the two random variables. If this intersection is unknown, then it is neglected and

$$P(A \cup B) \leq P(A) + P(B) \quad (76)$$

This is the union bound for the union of two random variables A and B [REF 6]. For the system considered in this thesis, the union bound gives

$$P_s \leq P(z_1 < z_2) + P(z_1 < z_3) + \dots + P(z_1 < z_M) \quad (77)$$

Since the  $z_m$ 's for  $m \neq 1$  are identical random variables, Equation (76) simplifies to

$$P_s \leq (M-1) P(z_1 < z_m) \quad (78)$$

The union bound gives an upper bound on  $P_e$ ; hence the results obtained are overly pessimistic.

There are two cases to consider in obtaining  $P(z_1 < z_m)$ . In case one,  $q_1 = x_{11}$ . In case two,  $q_1 = x_{i1}$  where  $i \neq 1$ . Now

$$P(z_1 < z_m) = P(z_1 - z_m < 0) = P(y_m < 0) \quad (79)$$

where

$$y_m = \sum_{l=1}^L y_{ml} \quad (80)$$

and

$$y_{ml} = z_{1l} - z_{ml} = \frac{x_{1l} - x_{ml}}{q_1} \quad (81)$$

By defining  $y_m$  this way, the analysis is similar to the binary case.

When  $q_1 = x_{11}$ ,

$$y_{ml} = 1 - \frac{x_{ml}}{x_{1l}} \quad (82)$$

and the pdf obtained for  $y_{ml}$  when  $0 \leq y_{ml} \leq 1$  is the same as in the binary case. When  $q_1 \neq x_{11}$ , the situation is more complicated.

If  $q_1 = x_{i1}$ , then

$$y_{m1} = \frac{x_{11}}{x_{m1}} - 1 \quad (83)$$

and

$$y_{i1} = \frac{x_{11}}{x_{m1}} - \frac{x_{i1}}{x_{m1}} \quad (84)$$

where  $i \neq 1, m$ . Clearly,

$$P(z_1 < z_m) \geq P(z_1 < z_i) \quad (85)$$

Hence, the use of Equation (82) to obtain the pdf for  $y_{m1}$  when  $-1 \leq y_{m1} < 0$  yields an upper bound to the union bound and leads to a pdf for  $y_{m1}$  that is identical to that obtained in the binary case.

The union bound is expected to be loose enough that the  $M$ -ary results are anomalous [REF 12]. The union bound becomes looser as  $M$  increases giving the false impression that performance decreases as  $M$  increases. This phenomenon will be taken into account in Chapter IV when the results are analyzed.

## 2. Converting From Bit Error to Symbol Error

In the binary case, the energy on a given branch is the bit energy because each branch represents a different bit. In the  $M$ -ary case, each branch represents a symbol and not a

bit. Therefore, the bit energy is some fraction of the energy carried on a branch and related to the value of  $M$  by

$$E_s = (\log_2 M) E_b \quad (86)$$

where  $E_s$  is the energy per symbol and  $E_b$  is the energy per bit. The analysis takes this difference into account in order to get correct results.

Another difference that is taken into account is the difference between bit error and symbol error. The transformation is

$$P_b = \frac{M/2}{M-1} P_s \quad (87)$$

where  $P_s$  is the probability of symbol error and  $P_b$  is the probability of bit error [REF 3].

Substituting Equation (77) into Equation (86) yields

$$P_b(E_b) = \left( \frac{M}{2} \right) P_s(E_s) \quad (88)$$

## F. PROBABILITY OF BIT ERROR

The final step in the derivation process is to obtain the pdf for the random variable  $w$  in Figure 3.1. The pdf of the independent random variables is the convolution of pdf's of the random variables comprising the sum. Hence

$$f_w(w) = [f_{y_1}^j(y_1)]^{\otimes j} \otimes [f_{y_1}^o(y_1)]^{\otimes (L-j)} \quad (89)$$

where the first term is the pdf for the jammed hops denoted by the  $j$  superscript and the second term is the pdf for the unjammed hops denoted by the  $o$  superscript. Once  $f_w(w)$  is obtained, Equation (4) is evaluated to obtain the probability of bit error. However, the multiple convolutions of Equations (39) and (40) or Equations (50) and (51) cannot in general be evaluated analytically and the remainder of the analysis is done numerically. Chapter IV describes the numerical procedure used to arrive at the probability of bit error.



## IV. NUMERICAL RESULTS

### A. NUMERICAL PROCEDURE

In Chapter III, the final result of the analysis is the probability density function for the random variable  $y_1$ . An example of  $f_{y_1}(y_1)$  is illustrated in Figure 4.1 for an envelope detector when the bit energy-to-noise density ratio ( $E_b/N_o$ ) is 13.35 dB, the direct-to-diffuse ratio is 10, and the bit energy-to-jammer density ratio ( $E_b/N_j$ ) is 20 dB. The function peaks when  $y_1$  is near 0.75. The function approaches zero when  $y_1$  approaches -1 or +1. For slow hopping, an error occurs when  $y_1$  is negative. In this case, the probability of  $y_1$  being negative is low. Figure 4.2 is an example for a bit energy-to-jammer density ratio of 3 dB. In this case, the probability of  $y_1$  being negative is much higher and the system performance is worse.

For fast frequency-hopping, the pdf of  $y_1$  must be convolved multiple times. Since the convolutions of Equation (88) cannot in general be done analytically, they are done numerically using MATLAB. The first step is to sample  $f_{y_1}(y_1)$  uniformly from -1 to +1 to obtain an array of numbers that can be operated on numerically. It was determined that 175 samples or greater is sufficient to get good results.

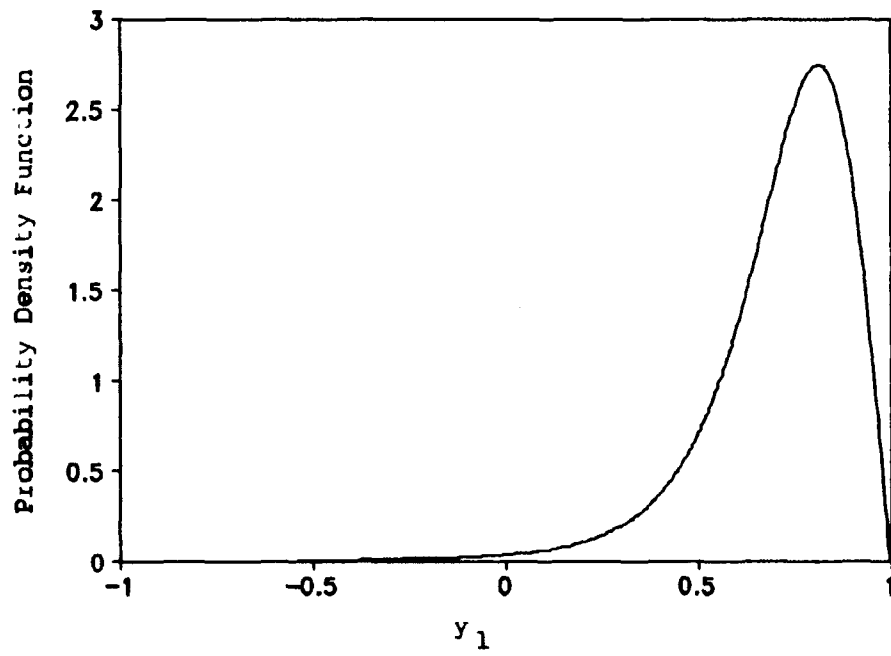


**Figure 4.1:**  $f_{y_1}(y_1)$  where  $E_b/N_o=13.35\text{dB}$ ,  $E_b/N_j=20\text{dB}$ ,  
Direct/Diffuse=10,  $\gamma=.25$

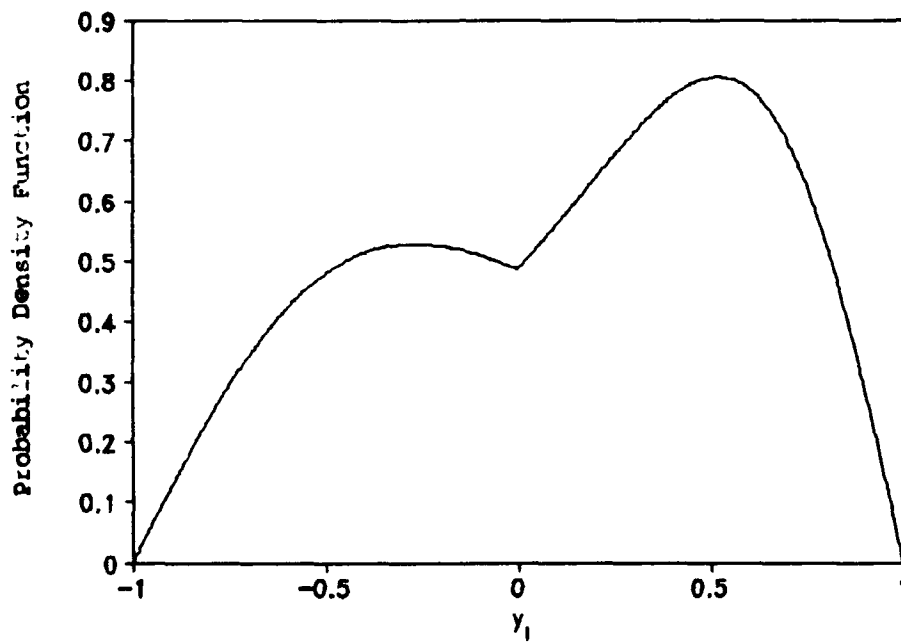


**Figure 4.2:**  $f_{y_1}(y_1)$  where  $E_b/N_o=13.35\text{dB}$ ,  $E_b/N_j=3\text{dB}$ ,  
Direct/Diffuse=10,  $\gamma=.25$

The next step in the analysis is to perform the operations in Equation (88) to obtain  $f_w(w)$  which is then integrated as shown in Equation (4) to obtain the probability of bit error.

Several parameters are varied in order to analyze system performance in different situations. The different parameters are:

- The direct-to-diffuse power ratio is varied to examine the effects of Rician fading on the system.
- The bit energy-to-jammer density ratio is varied to examine the effects of jamming on the system.
- The diversity ( $L$ ) is varied.
- The bit energy-to-noise density ratio is varied to measure the effects of wideband noise on the system.
- The number of bits per symbol ( $M$ ) is varied to examine the change in performance.
- The jamming duty factor ( $\gamma$ ) is varied to measure the effects of different amounts of partial-band jamming on the system.

By varying these parameters, several different approaches can be taken to determine system performance.

## **B. BFSK ENVELOPE DETECTOR**

### **1. $E_b/N_0 = 16$ dB**

Figure 4.3 is a plot of the effects of fading on system performance. Only thermal noise is present in Figure 4.3, so the difference in performance is due to Rician fading and nonlinear combining losses. The bit energy-to-noise density ratio is fixed at 16 dB. As shown in Figure 4.3,

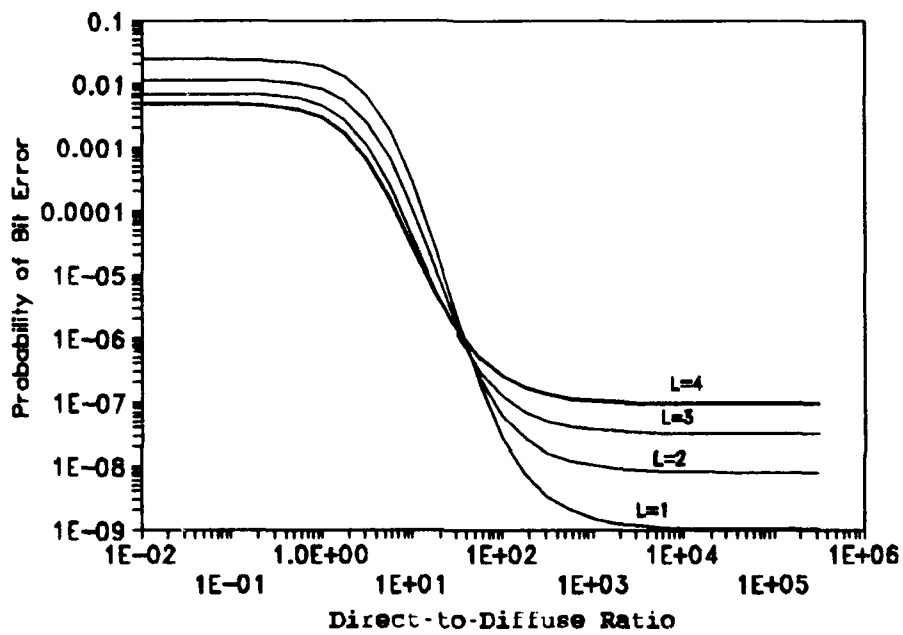


**Figure 4.3: Probability of Bit Error Versus Direct-to-Diffuse Ratio for a BFSK Receiver with Envelope Detection where  $E_b/N_0=16\text{dB}$ , No Jamming**

Rician fading must be accounted for in system performance. The probability of bit error drops an average of three decades from the Rayleigh limit to the non-faded channel limit. At the Rayleigh limit, increased diversity counteracts the affects of fading which dominates receiver performance in this region. At a direct-to-diffuse ratio of 10, nonlinear combining losses begin to dominate and diversity becomes a disadvantage. At a direct-to-diffuse ratio of 1000, the channel is essentially non-faded and nonlinear combining losses dominate receiver performance. For values of the direct-to-diffuse ratio where performance is essentially constant as the direct-to-diffuse ratio changes, a change in the amount of fading does not significantly change the probability of bit error even when partial-band jamming is present. In this thesis, the performance of the system in the presence of partial-band jamming is examined for direct-to-diffuse ratios of .01, 10, and 10000 which correspond to both of the asymptotic regions as well as the transition region.

Figures 4.4-4.7 are illustrations of the receiver performance for specific fractions of partial-band jamming as well as worst case partial-band jamming at a ratio of 10 for diversities of 1,2,3 and 4, respectively. Worst case performance implies that the specific fraction of partial-band jamming is at the value where the bit energy-to-jammer density ratio is most effective. The worst case occurs at the point where the probability of bit error begins to reach its

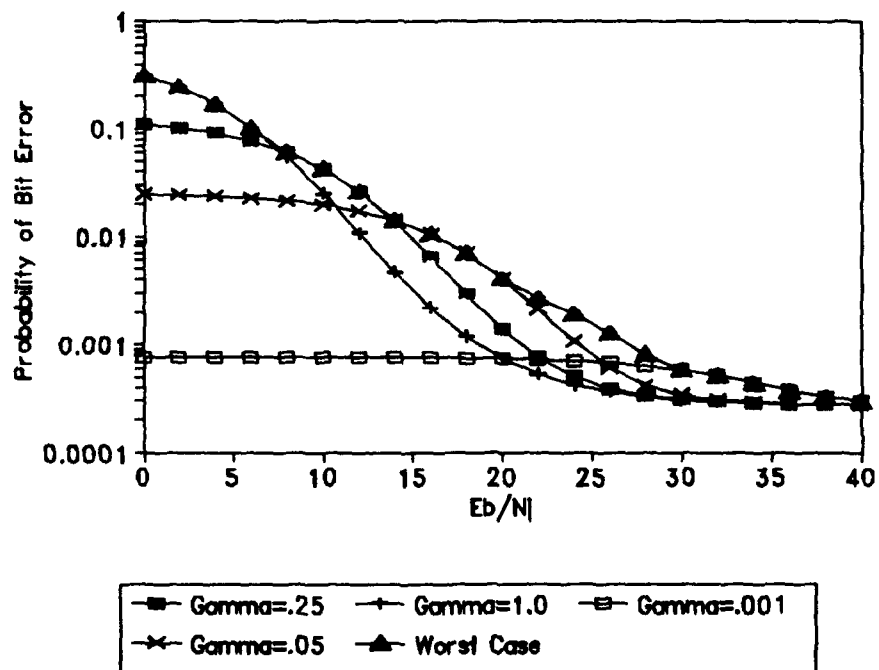


**Figure 4.4: Performance of a BFSK Receiver with Envelope Detection where  $E_b/N_0=16\text{dB}$ , Direct/Diffuse=10, and  $L=1$**

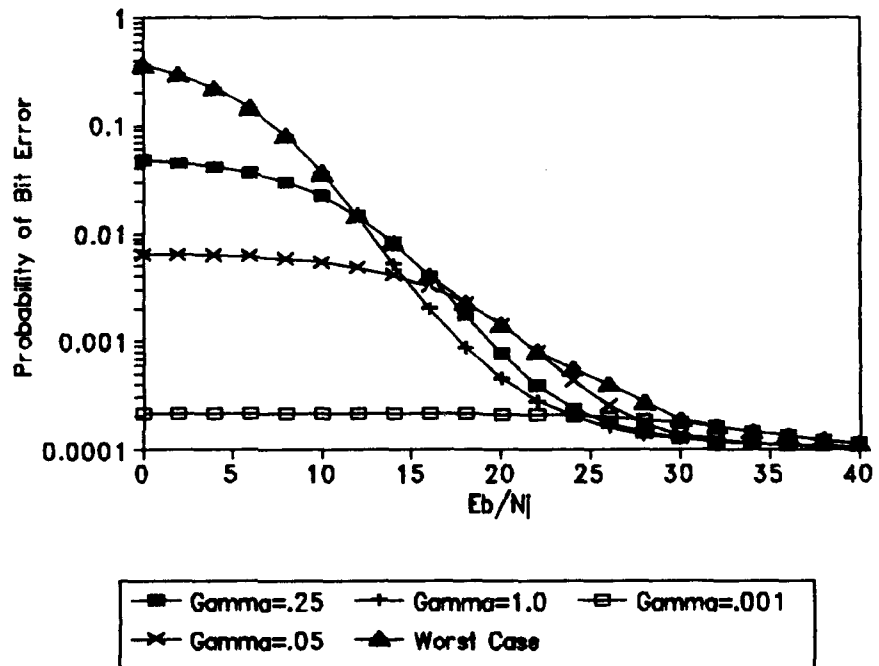
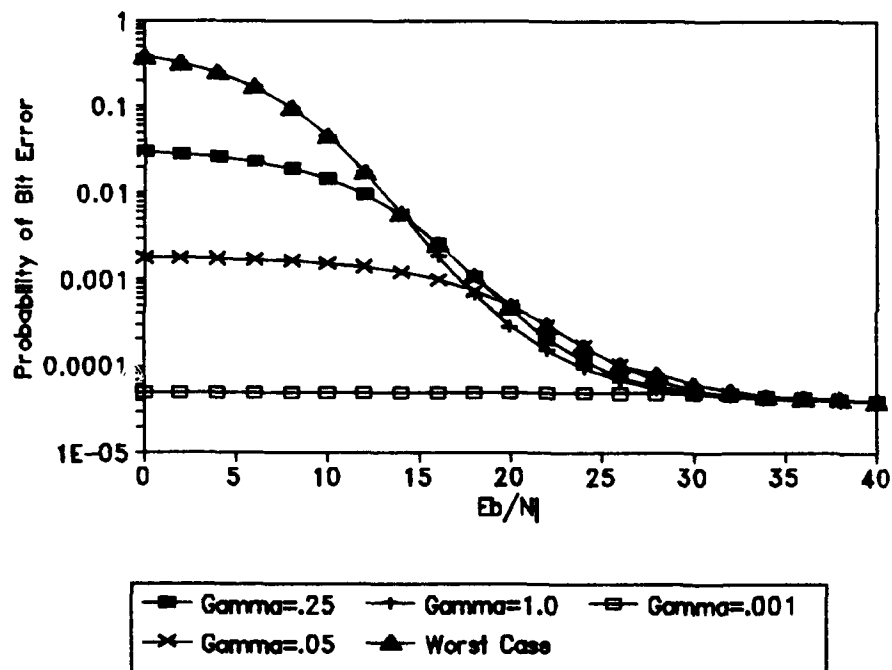
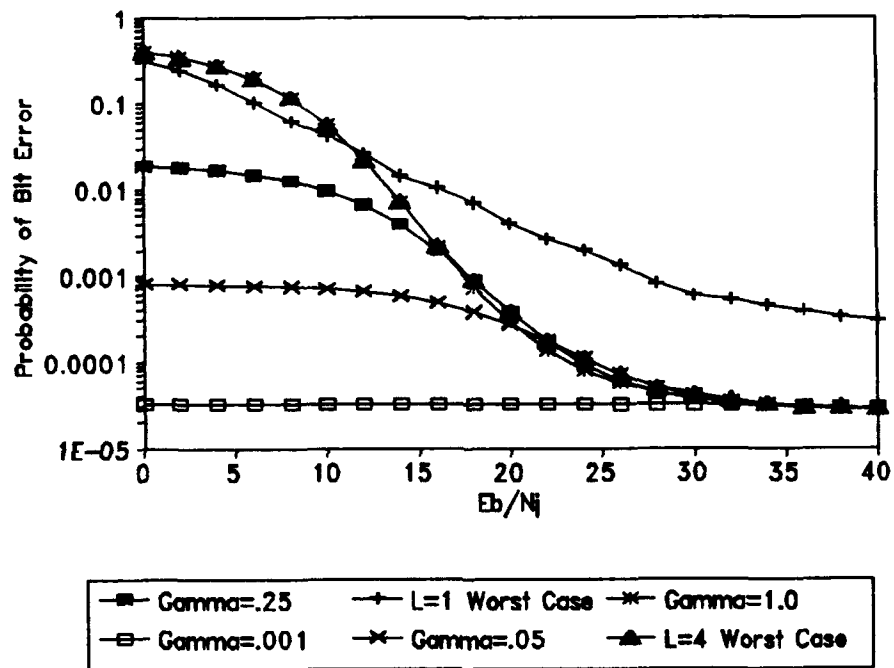


Figure 4.5: Performance of a BFSK receiver with Envelope Detection where  $E_b/N_0=16\text{dB}$ , Direct/Diffuse=10, and  $L=2$





**Figure 4.6: Performance of a BFSK Receiver with Envelope Detection where  $E_b/N_0=16\text{dB}$ , Direct/Diffuse=10, and  $L=3$**



**Figure 4.7: Performance of a BFSK Receiver with Envelope Detection where  $E_b/N_0=16\text{dB}$ , Direct/Diffuse=10, and  $L=4$  with  $L=1$  worst case**

greatest negative slope. System performance for all of the different fractions of partial-band jamming reach a lower limit at the point where the effects of thermal noise dominate. For small fractions of partial-band jamming, the system performs better except for higher bit energy-to-jammer density ratios. In Figure 4.4, the broad band jamming performance is better than the 25% partial-band jamming for bit energy-to-jammer density ratios greater than 8 dB. From 8 dB to 40 dB, the use of partial-band jamming results in a significant degradation of receiver performance. It is interesting to note that for bit energy-to-jammer density ratios less than 8 dB, receiver performance improves dramatically when the interference is partial-band rather than uniform for a given interference power spectral density. It can be seen that, in certain cases, the jammer can use less power and a less complex transmitter (i.e., uniform instead of partial-band jamming) to achieve the same degradation in receiver performance. As can be seen in Figure 4.5, the degradation in receiver performance due to partial-band jamming is significantly reduced for  $L=2$  and is further reduced for  $L=3$  as shown in Figure 4.6. In Figure 4.7, the worst case performance occurs when the interference is uniform for all values of bit energy-to-jammer density ratio except for a narrow region at 25 dB. Hence, for a direct-to-diffuse ratio of 10 and a bit energy-to-noise density ratio of 16 dB, the performance of the BFSK fast-frequency hopped, ratio-

statistic receiver with envelope detection is virtually immune to degradation caused by partial-band jamming when at least 4 hops are used.

As can be seen in Figure 4.4-4.7, the worst case performance with no diversity is substantially poorer than the worst case performance in the other three cases for relatively high values of interference. Figure 4.7 includes a plot of the worst case performance for  $L=1$  for ease of comparison. As can be seen in Figure 4.7, there is an improvement in performance when a diversity of four is used for bit energy-to-jammer density ratios above 13 dB.

Figure 4.8 illustrates the effect of partial-band jamming on receiver performance in the presence of a non-faded channel with no diversity. The degradation due to partial-band jamming is much more dramatic for the non-faded channel.

Figure 4.9 illustrates the effect of diversity on receiver performance in the presence of Rayleigh fading. As can be seen, the effect of diversity is advantageous, but less dramatic than for higher direct-to-diffuse ratios.

Figure 4.10 is another illustration of the effect of fading on receiver performance. Figure 4.10 includes a plot of worst case performance at each of the regions in Figure 4.3 for  $L=4$ . As can be seen, fading has a significant effect for bit energy-to-jammer density ratios above 10 dB and must be taken into account.

## 2. $E_b/N_0 = 13.35$ dB

Figures 4.11-4.14 are illustrations of the receiver performance for specific fractions of partial-band jamming as well as worst case partial-band jamming at a direct-to-diffuse ratio of 10 for diversities of 1,2,3 and 4, respectively. In Figure 4.11, the broad band jamming performance is better than the 25% partial-band jamming for bit energy-to-jammer density ratios greater than 7 dB. When the bit energy-to-jammer density ratio is greater than 35 dB, broad-band jamming is again the worst case. From 7 dB to 35 dB, the use of partial-band jamming results in a significant degradation of receiver performance. This degradation is less severe than for a bit energy-to-noise density of 16 dB as can be seen by comparing Figures 4.4 and 4.11. As can be seen in Figure 4.12, the degradation in receiver performance due to partial-band jamming is significantly reduced for  $L=2$  and is virtually eliminated when  $L=3$  as shown in Figure 4.13. As can be seen in Figure 4.14, the worst case performance occurs when the interference is uniform for all values of bit energy-to-jammer density ratio. Hence, for a direct-to-diffuse ratio of 10 and a bit energy-to-noise density ratio of 13.35 dB, the performance of the BFSK fast-frequency hopped, ratio-statistic receiver with envelope detection is immune to degradation caused by partial-band jamming when at least 3 hops are used.

As can be seen in Figure 4.11-4.14, the worst case performance with no diversity is significantly worse than the

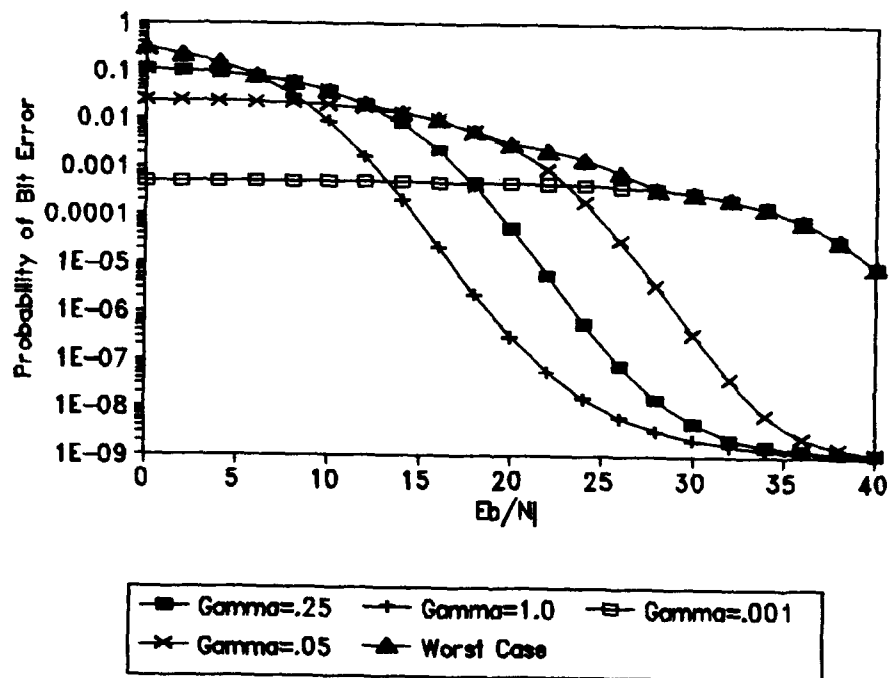
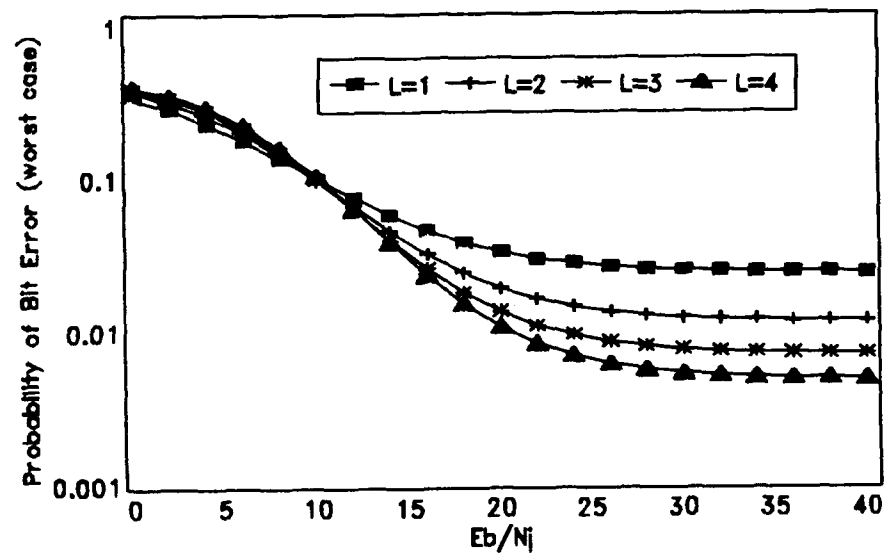
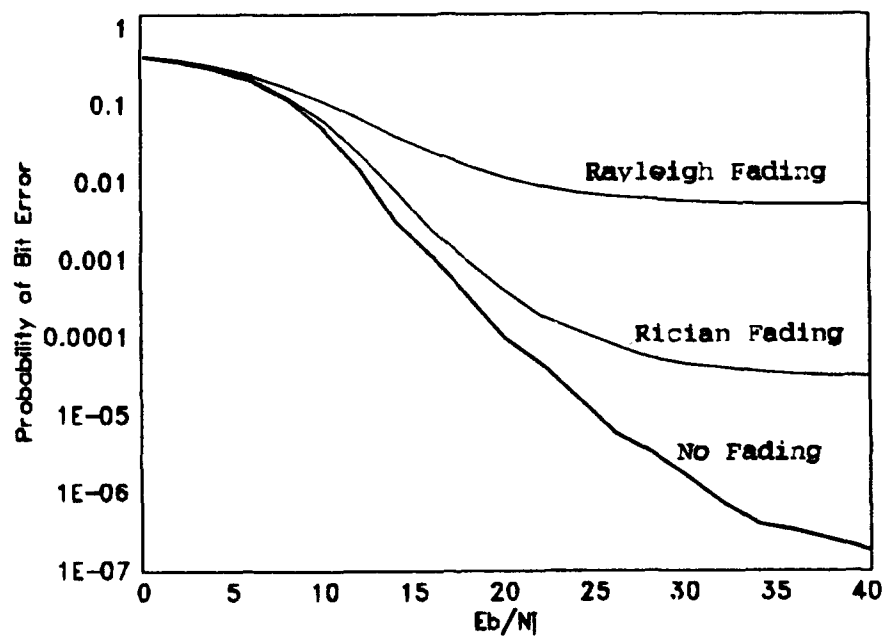


Figure 4.8: Performance of a BFSK Receiver with Envelope Detection where  $E_b/N_0=16\text{dB}$ , Direct/Diffuse=10000, and :



**Figure 4.9: Worst Case Performance of a BFSK Receiver with Envelope Detection where  $E_b/N_0=16\text{dB}$ , Direct/Diffuse=.01, and  $L=1,2,3$  and 4.**



**Figure 4.10: Worst Case Performance of a BFSK Receiver with Envelope Detection where  $E_b/N_0=16\text{dB}$  and  $L=4$  for Different Amounts of Fading**



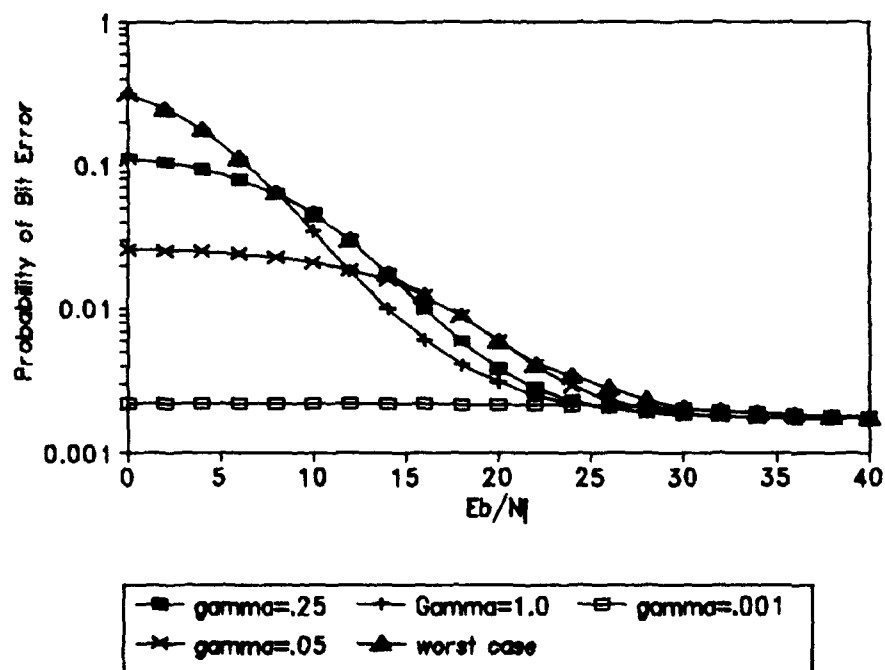
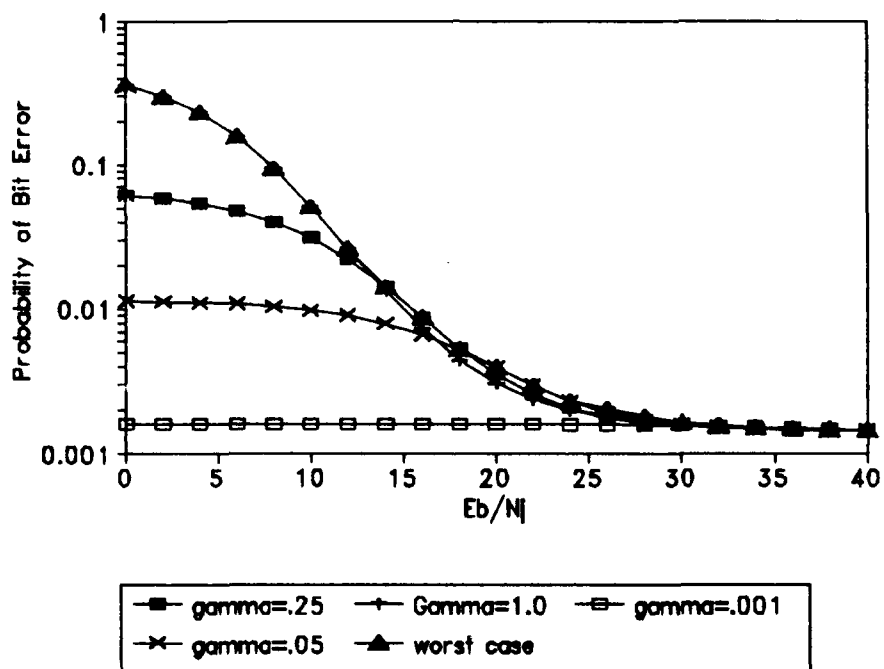
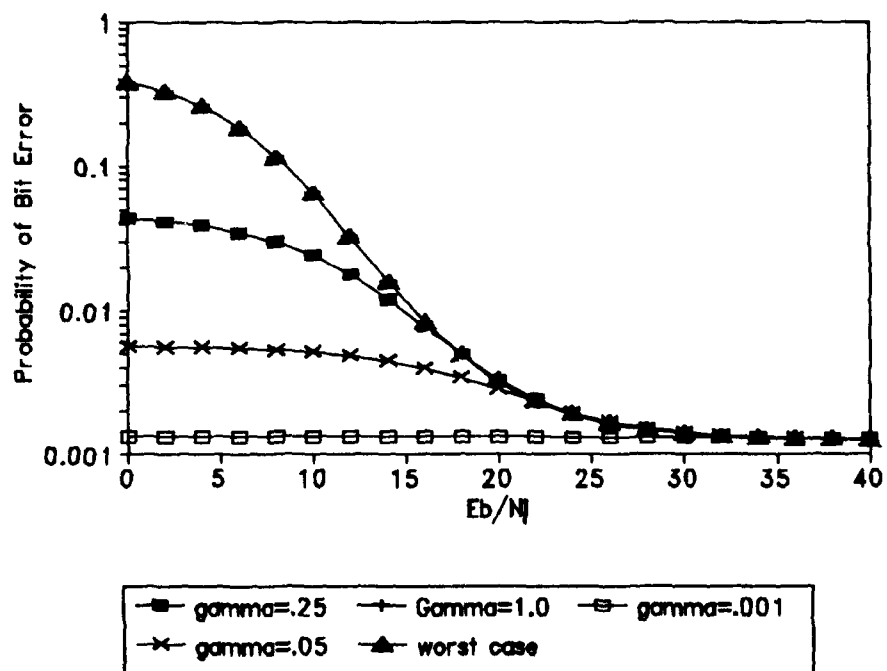


Figure 4.11: Performance of a BFSK Receiver with Envelope Detection where  $E_b/N_0=13.35\text{dB}$ , Direct/Diffuse=10, and  $L=1$



**Figure 4.12: Performance of a BFSK Receiver with Envelope Detection where  $E_b/N_0=13.35\text{dB}$ , Direct/Diffuse=10, and  $L=2$**



**Figure 4.13: Performance of a BFSK Receiver with Envelope Detection where  $E_b/N_0=13.35\text{dB}$ , Direct/Diffuse=10, and  $L=3$**

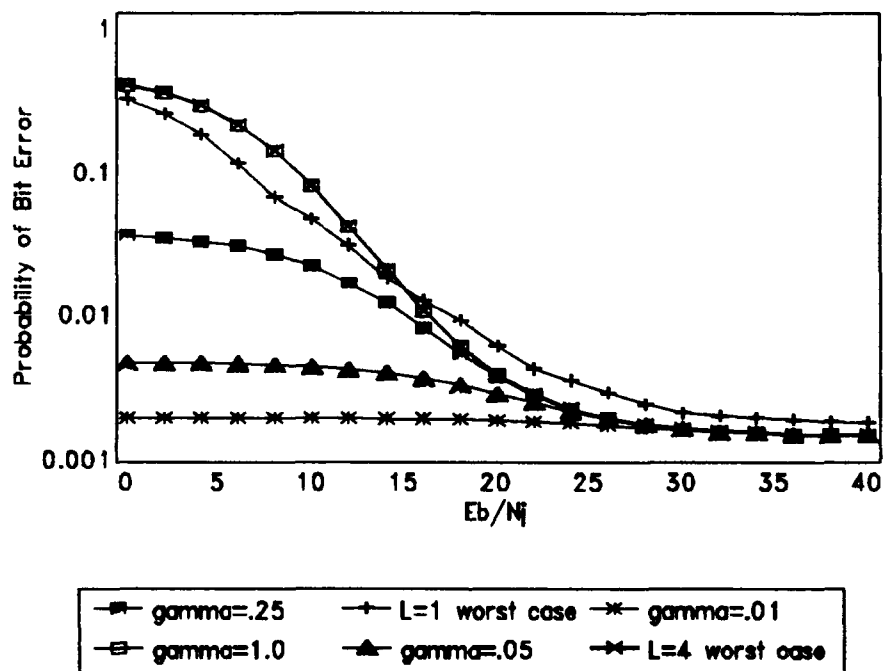


**Figure 4.14: Performance of a BFSK Receiver with Envelope Detection where  $E_b/N_0=13.35\text{dB}$ , Direct/Diffuse=10, and  $L=4$  with  $L=1$  worst case**

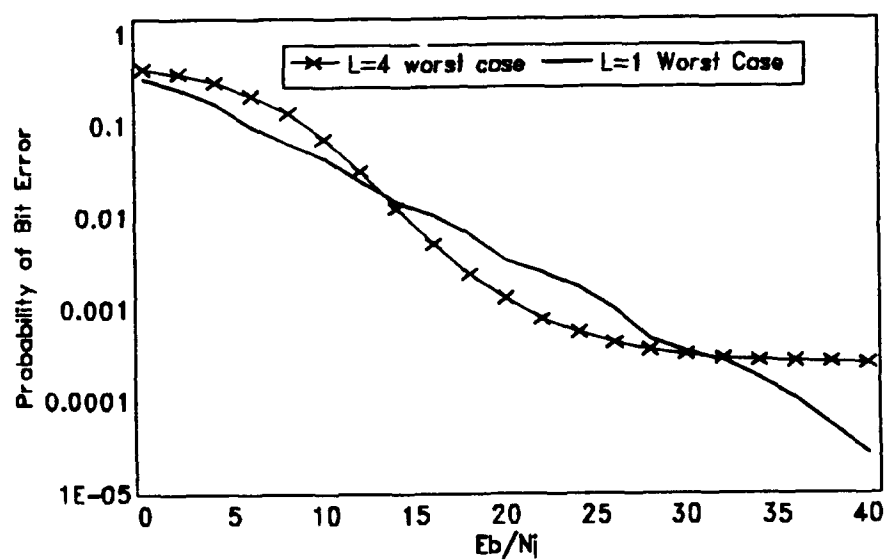


**Figure 4.15: Performance of a BFSK Receiver with Envelope Detection where  $E_b/N_0=13.35\text{dB}$ , Direct/Diffuse=10000, and  $L=1$  and 4.**

worst case performance in the other three cases for relatively high values of interference. Figure 4.14 includes a plot of the worst case performance for  $L=1$  for ease of comparison. As can be seen in Figure 4.14, there is an improvement in performance when diversity is used for bit energy-to-jammer density ratios above 15 dB. For a non-faded channel, the performance advantage due to increased diversity is lost at bit energy-to-jammer density ratios greater than 30 dB. This is illustrated in Figure 4.15 where the  $L=1$  worst case performance drops below the  $L=4$  worst case plot.

Figure 4.16 is an illustration of the worst case performance for  $L=1, 3$ , and  $4$  for both bit energy-to-noise density ratios of 13.35 dB and 16 dB and a direct-to-diffuse ratio of 10. It can be seen that performance begins to improve as the bit energy-to-jammer density ratio becomes larger than the bit energy-to-noise density ratio. At this point thermal noise begins to dominate performance, and the probability of bit error approaches an asymptotic lower limit dictated by the bit energy-to-noise density ratio. When the bit energy-to-jammer density ratio is very large, performance is completely dominated by thermal noise and does not change significantly for small changes in bit energy-to-jammer density ratio. Since receiver performance for a bit energy-to-noise density ratio of 13.35 dB is worse than for a bit energy-to-noise density ratio of 16 dB, the probability of bit error in the presence of a higher bit energy-to-noise

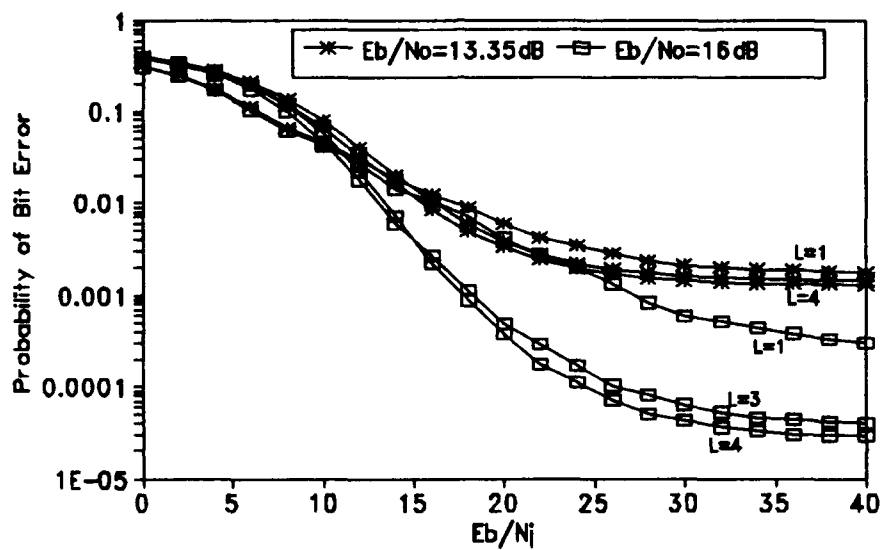


**Figure 4.16: Comparison of the Performance of a BFSK Receiver with Envelope Detection where Direct/Diffuse=10 for  $E_b/N_o=13.35 \text{ dB}$  versus  $16 \text{ dB}$**

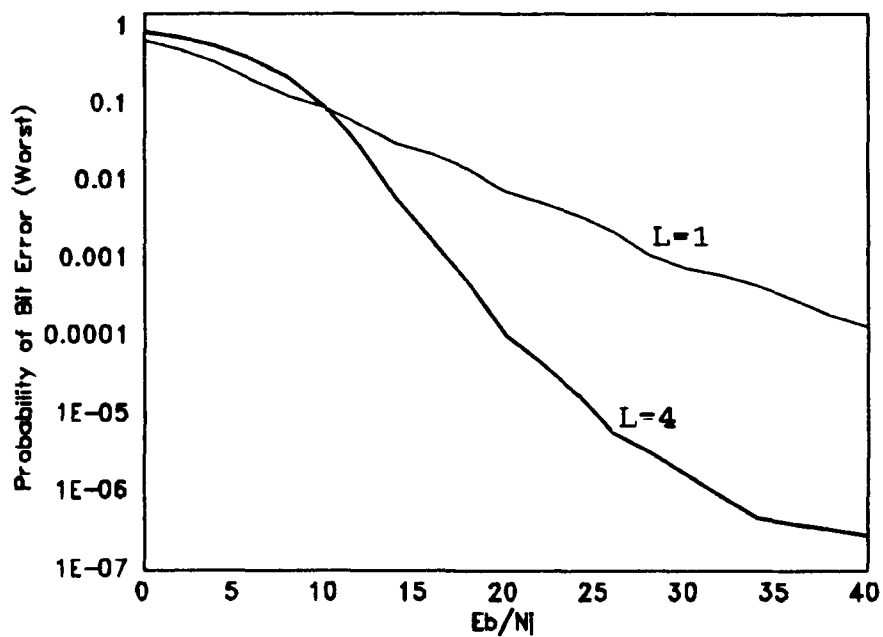
density ratio drops off sooner and diversity is advantageous at a lower bit energy-to-jammer density ratio. Also, it can be seen from Figure 4.16 that the receiver performance for  $L=4$  is much better than for  $L=1$  for a bit energy-to-noise density ratio of 16 dB, but only marginally so for a signal-to-thermal ratio of 13.35 dB. As is expected, the receiver performance is always better for a higher bit energy-to-noise density ratio.

### C. M-ARY ENVELOPE DETECTOR

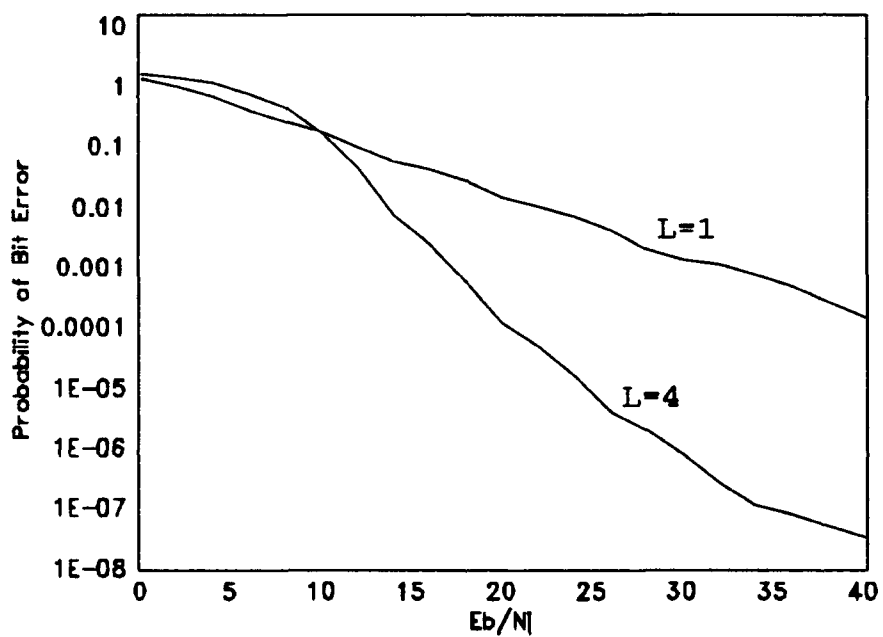
Figure 4.17 is an illustration of the effect of diversity on a 4-ary FSK receiver in the presence of a bit energy-to-noise density ratio of 16 dB and a direct-to-diffuse ratio of 10. It can be seen from Figure 4.17 that higher diversity gives better receiver performance for bit energy-to-jammer density ratios greater than 13 dB. By comparing Figure 4.17 with Figure 4.7, one sees that the advantage of higher diversity in receiver performance is more dramatic in the 4-ary FSK receiver than the BFSK receiver. This is also true as  $M$  increases to 8-ary FSK and to 16-ary FSK as can be seen in Figures 4.18 and 4.19.

Figures 4.20 - 4.22 illustrate the effect of diversity on receiver performance in the presence of Rayleigh fading for  $M=4, 8$ , and 16. By comparing Figures 4.20 - 4.22 with Figure 4.10, one can see that the advantage of diversity increases as  $M$  increases for Rayleigh fading.

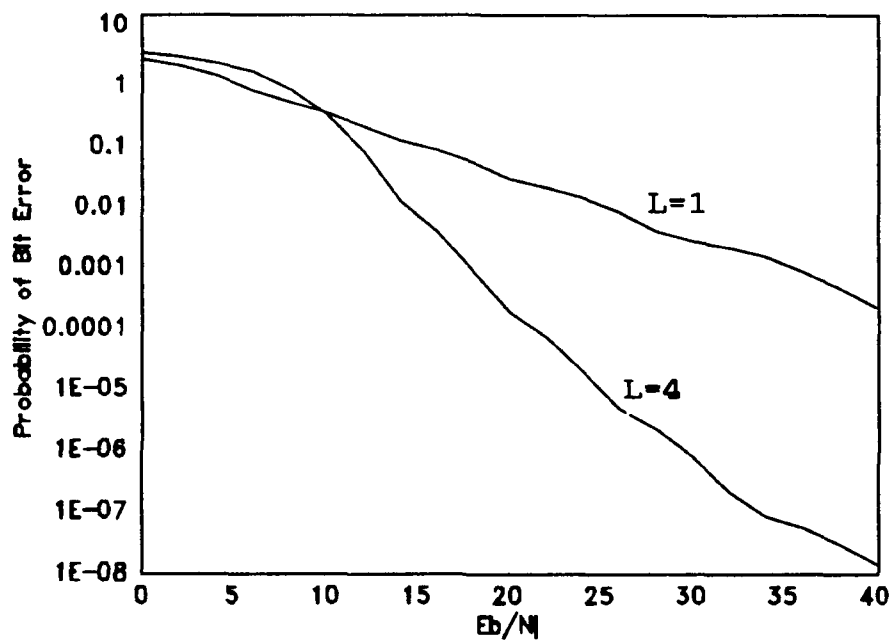




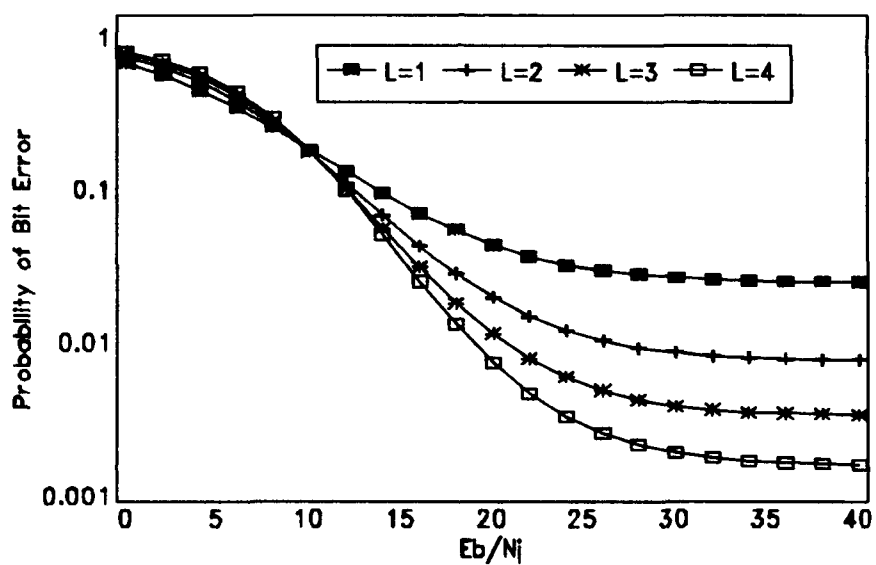
**Figure 4.17: Worst Case Performance of a 4-ary FSK Receiver with Envelope Detection where  $E_b/N_0=16$ dB, Direct/Diffuse=10, and  $L=1$  and 4**



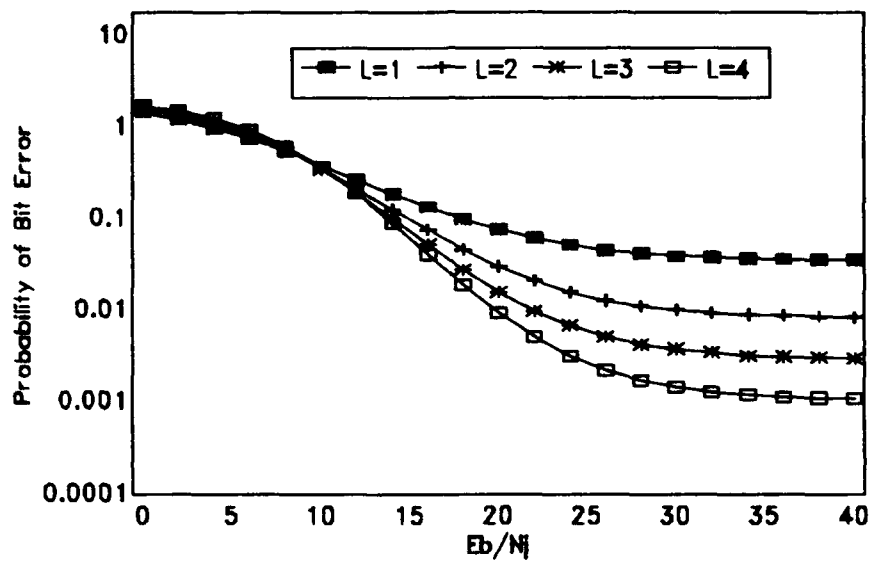
**Figure 4.18: Worst Case Performance of an 8-ary FSK Receiver with Envelope Detection where  $E_b/N_0=16\text{dB}$ , Direct/Diffuse=10, and  $L=1$  and 4**



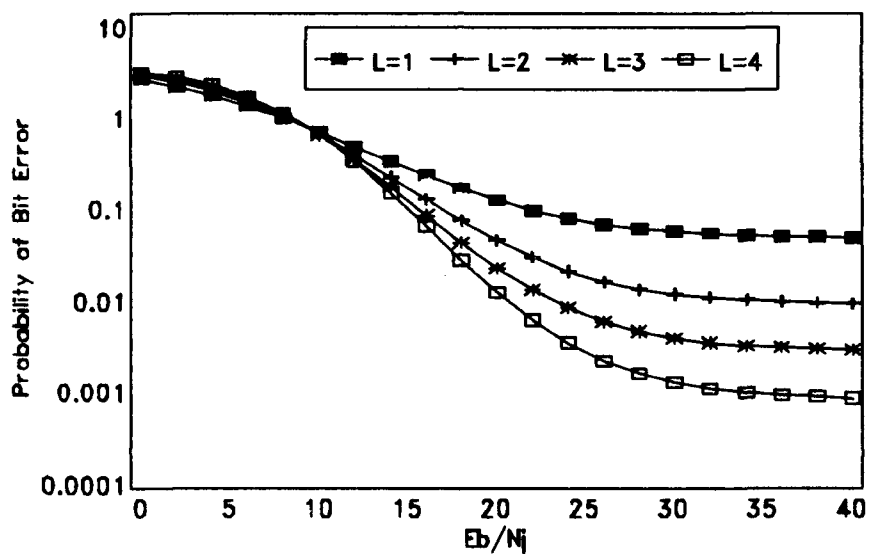
**Figure 4.19: Worst Case Performance of a 16-ary FSK Receiver with Envelope Detection where  $E_b/N_0=16\text{dB}$ , Direct/Diffuse=10, and  $L=1$  and 4**



**Figure 4.20: Worst Case Performance of a 4-ary FSK Receiver with Envelope Detection where  $E_b/N_o=16\text{dB}$ , Direct/Diffuse=.01, and  $L=1-4$**



**Figure 4.21: Worst Case Performance of an 8-ary FSK Receiver with Envelope Detection where  $E_b/N_0=16\text{dB}$ , Direct/Diffuse=.01, and  $L=1-4$**



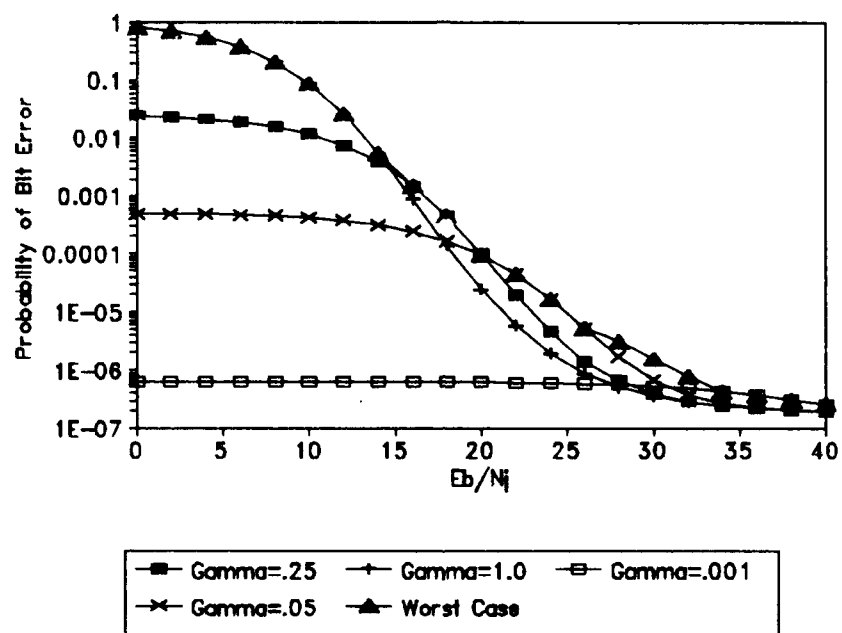
**Figure 4.22: Worst Case Performance of a 16-ary FSK Receiver with Envelope Detection where  $E_b/N_0=16\text{dB}$ , Direct/Diffuse=.01, and  $L=1-4$**

Figure 4.23 is an illustration of the immunity to partial-band jamming for a 4-ary FSK envelope detector receiver for  $L=4$  in the presence of a bit energy-to-noise density ratio of 16 dB. It can be seen that the 4-ary FSK receiver is not immune to partial-band jamming at  $L=4$  as is the BFSK receiver as shown in Figure 4.7; although, the performance of the 4-ary FSK receiver is better than the BFSK receiver for bit energy-to-jammer density ratios greater than 13 dB as shown in Figure 4.24.

Figures 4.25 illustrates the effect of partial-band interference on receiver performance at the non-faded limit for an 8-ary FSK receiver. By comparing Figure 4.25 to Figure 4.9, one sees that the degradation is more dramatic as  $M$  increases. This shows that the receiver is more sensitive to partial-band jamming as  $M$  increases.

Figure 4.24 is an illustration of the worst case performance for  $L = 4$  in an  $M$ -ary receiver for  $M = 2, 4, 8$ , and 16 in the presence of a bit energy-to-noise density of 16 dB and a direct-to-diffuse ratio of 10. It can be seen that, for high bit energy-to-jammer density ratios, the receiver performance improves as  $M$  increases. It is interesting to note that, for low bit energy-to-jammer density ratios, the receiver performance is better as  $M$  decreases.

Figure 4.26 is similar to Figure 4.16 with the exception that



**Figure 4.23: Performance of a 4-ary FSK Receiver with Envelope Detection where  $E_b/N_0=16\text{dB}$ , Direct/Diffuse=10, and  $L=4$**



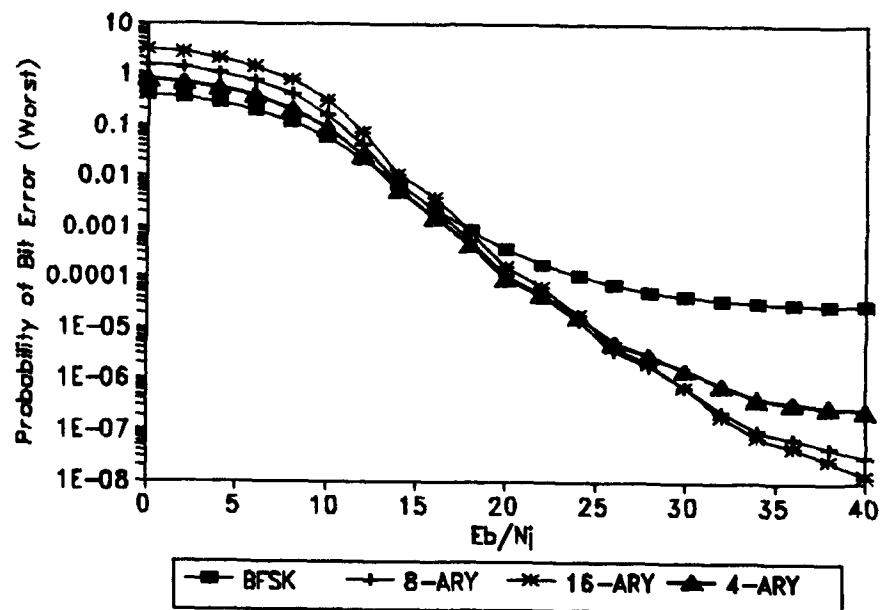


Figure 4.24: Performance of M-ary FSK Receivers with Envelope Detection where  $E_b/N_0=16\text{dB}$ , Direct/Diffuse=10,  $L=4$  and  $M=2, 4, 8$ , and 16

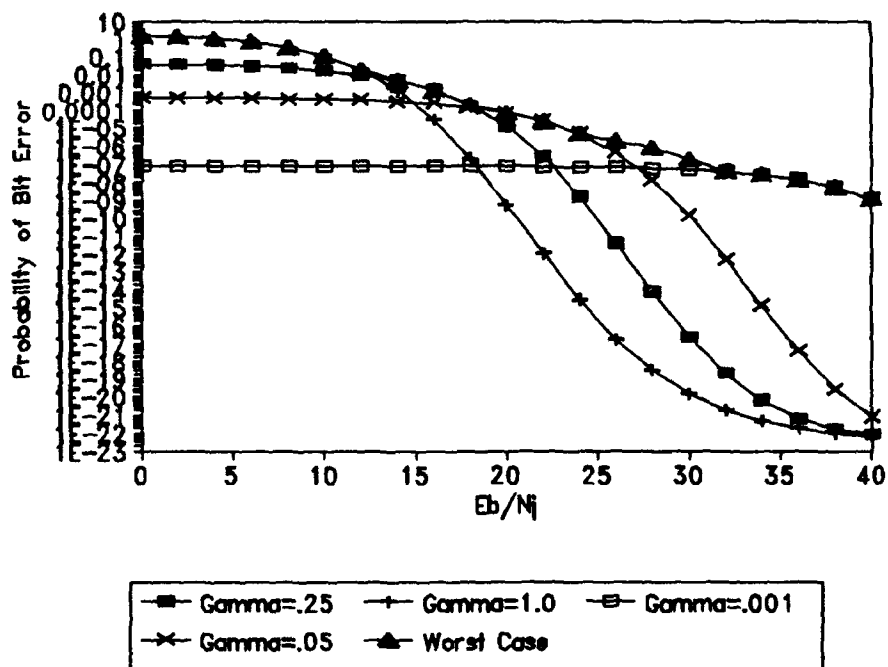
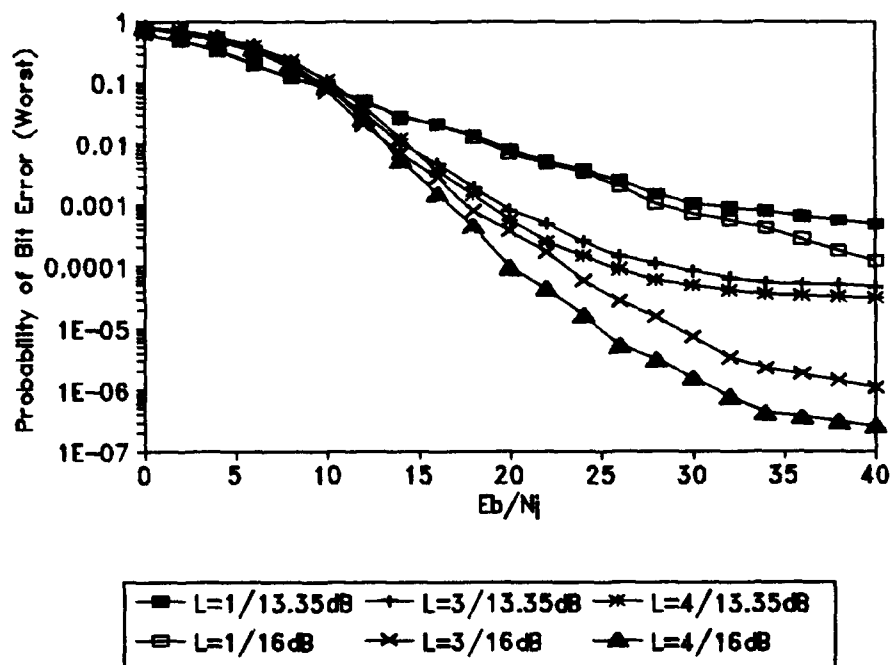


Figure 4.25: Performance of an 8-ary FSK Receiver with Envelope Detection where  $E_b/N_0=16\text{dB}$ , Direct/Diffuse=10000, and  $L=4$



**Figure 4.26: Performance of a 4-ary FSK Receiver with Envelope Detection where  $E_b/N_0=16$ dB, Direct/Diffuse=10 for  $E_b/N_0=13.35$  versus 16dB**

the receiver is 4-ary FSK instead of BFSK. It can be seen that the conclusions drawn from the results shown in Figure 4.26 are essentially the same as those drawn from the results in Figure 4.16. Receiver performance in the presence of a higher bit energy-to-noise density ratio is better and improves sooner as the bit energy-to-jammer density ratio increases than for a lower bit energy-to-noise density ratio. By comparison, it can be seen for the 4-ary FSK receiver, performance improves for lower bit energy-to-jammer density ratios than for the BFSK receiver and diversity becomes advantageous at an even lower bit energy-to-jammer density ratio.

Figures 4.27 - 4.30 examine the trade off of higher diversity versus higher values of  $M$ . As can be seen in Figure 4.27, at the Rayleigh limit and a bit energy-to-noise density ratio of 16 dB, a BFSK receiver with  $L=4$  out performs the  $M$ -ary receivers with no diversity. As can be seen in Figure 4.28, for a direct-to-diffuse ratio of 10 and a bit energy-to-noise density ratio of 16 dB, a BFSK receiver with  $L=4$  still out performs the  $M$ -ary receivers with no diversity except for a bit energy-to-jammer density ratio of less than 5 dB where a 4-ary FSK receiver has an equivalent performance. As can be seen in Figure 4.29, for a direct-to-diffuse ratio of 10 and a bit energy-to-noise density ratio of 13.35 dB, a 4-ary FSK receiver with no diversity performs better than a BFSK receiver with  $L=4$  except for bit energy-to-jammer density

ratios between 10 dB and 28 dB. As can be seen in Figure 4.30, for a non-faded channel and a bit energy-to-noise density ratio of 16 dB, the BFSK receiver with  $L=4$  outperforms the  $M$ -ary receivers with  $L=1$  except for bit energy-to-jammer density ratios less than 7 dB where the 4-ary FSK receiver is slightly better. It is interesting to note that, for all channels with  $M$ -ary FSK receivers, the system with  $L=1$  is more sensitive to partial-band interference than the BFSK receiver. The results in Figures 4.27 -4.30 are as expected for the union bound used to approximate the performance of the  $M$ -ary receivers [REF 12]. It is not the expected result for the actual performance and, therefore, the conclusion is made that the union bound for the  $M$ -ary receiver performance is too loose to do an accurate comparison. Receiver performance should always improve as  $M$  increases.

#### D. ENVELOPE DETECTOR VERSUS SQUARE-LAW DETECTOR

By comparing Figure 4.31 to Figure 4.1 and Figure 4.32 to Figure 4.2, one can see that the pdf for  $L=1$  in an envelope detector is quite different from that of a square-law detector. However, comparisons of the data for the ratio-statistic combining receivers between the envelope detector and square-law detector show that, for  $L=1$ , the receiver performance is exactly the same (as is proven in section III.D). The data also shows that, for  $L=2$ , the receiver performance is equivalent. Figure 4.33 is an illustration of

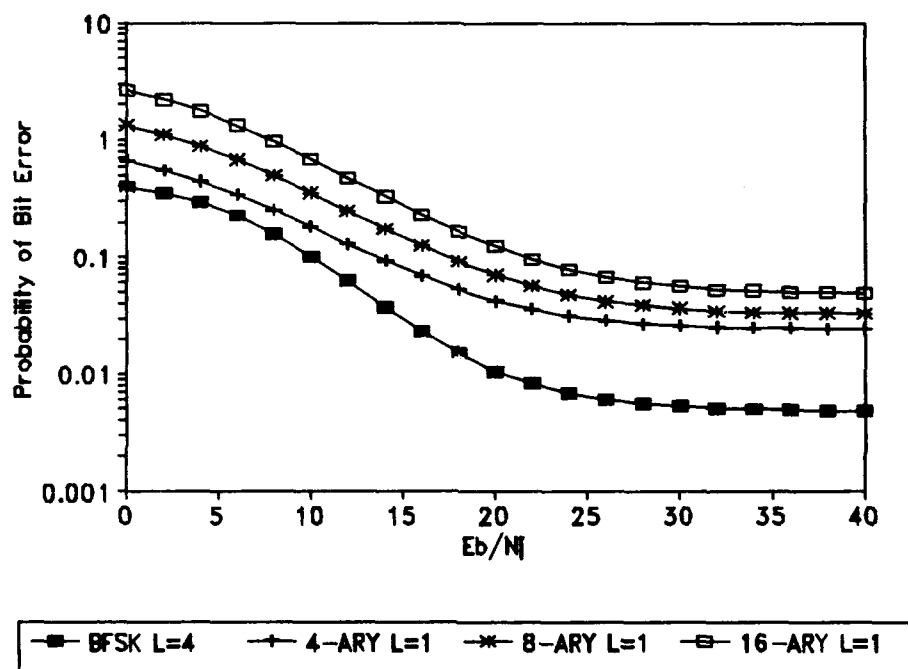


**Figure 4.27: Performance of BFSK Receiver with L=4 versus M-ary Receivers with L=1 where  $E_b/N_0=16\text{dB}$ , Direct/Diffuse=.01 and Envelope Detection**

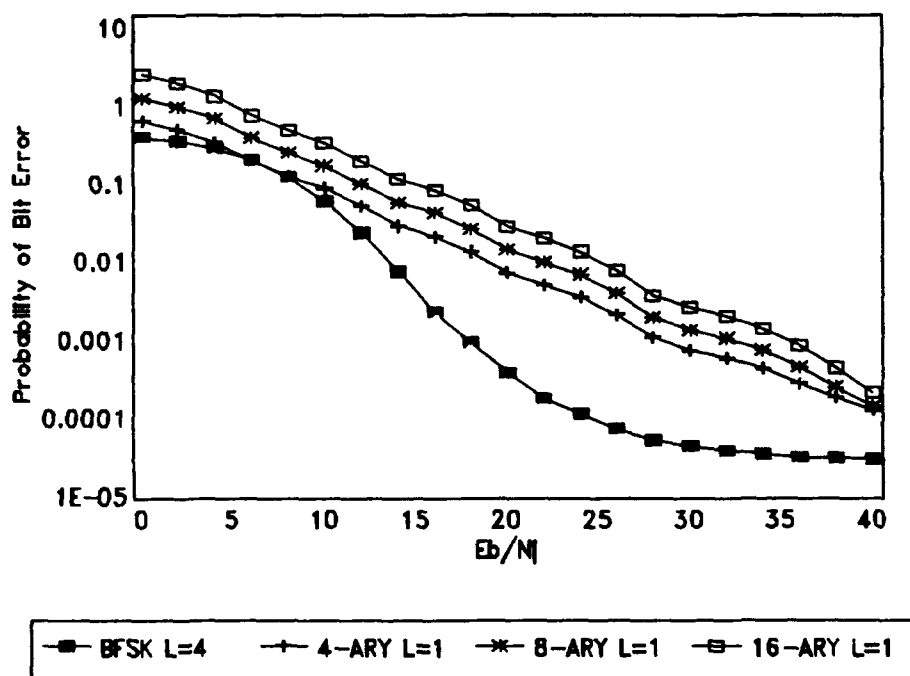


**Figure 4.28: Performance of a BFSK Receiver with  $L=4$  versus M-ary Receivers with  $L=1$  where  $E_b/N_0=16\text{dB}$ , Direct/Diffuse=10 and Envelope Detection**

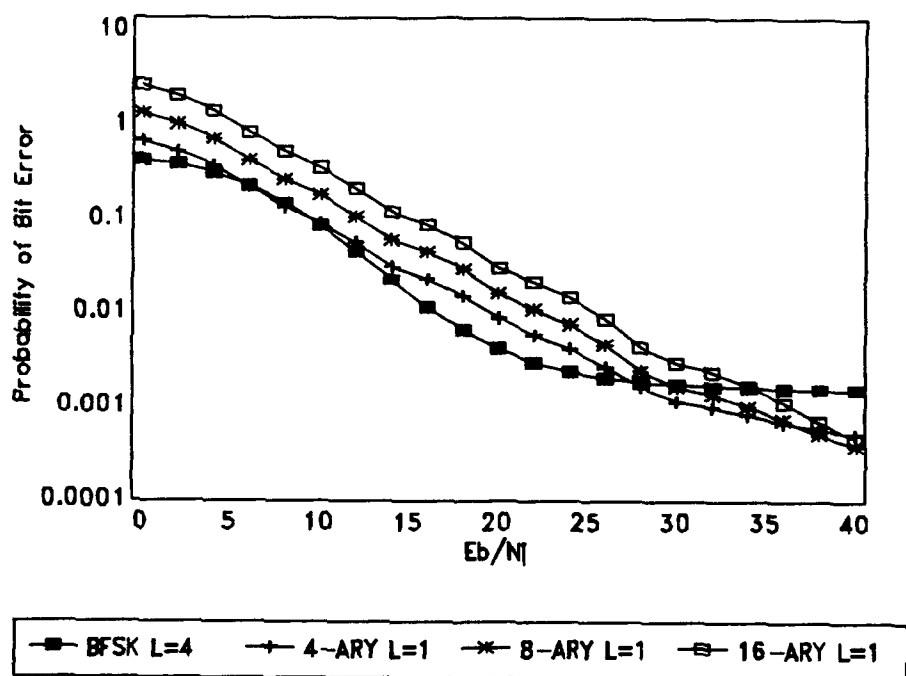


**Figure 4.29: Performance of a BFSK Receiver with  $L=4$  versus M-ary Receivers with  $L=1$  where  $E_b/N_0=13.35\text{dB}$ , Direct/Diffuse=10 and Envelope Detection**



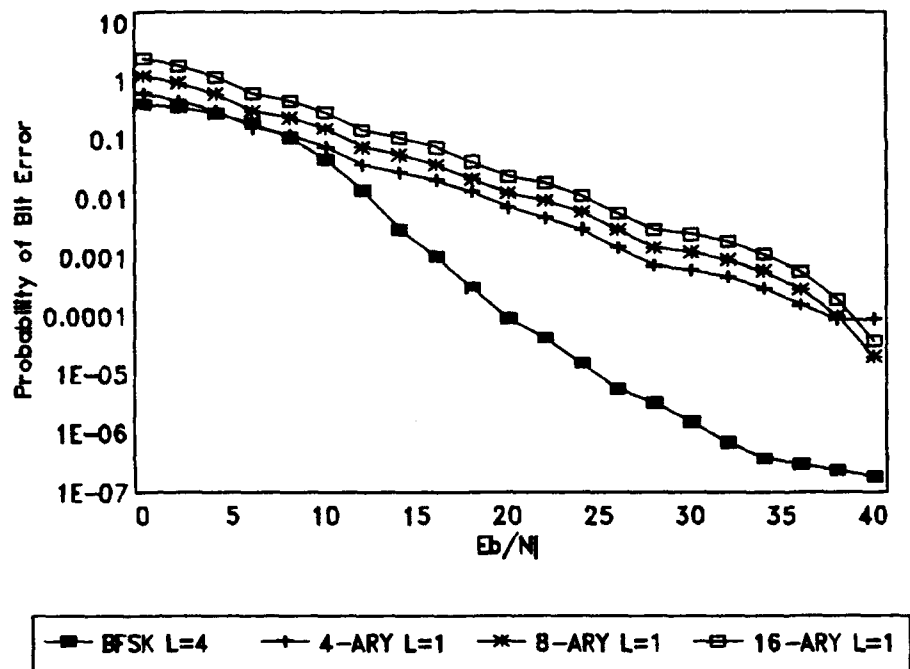


**Figure 4.30: Performance of a BFSK Receiver with  $L=4$  versus M-ary Receivers with  $L=1$  where  $E_b/N_0=16\text{dB}$ , Direct/Diffuse=10000 and Envelope Detection**

the worst case performances for  $L=1$  through 4 in a BFSK envelope detector and a square-law detector in the presence of a bit energy-to-noise density ratio of 16 dB and a direct-to-diffuse ratio of 10. As can be seen, for  $L=1$  and 2, the performance is identical. The difference arises when  $L$  is increased to three and four. From Figure 4.33, for  $L=3$  and 4, the envelope detector outperforms the square-law detector for the entire range of bit energy-to-jammer density ratios. Figure 4.34 is an illustration of the same receiver in the presence of a signal-to-thermal ratio of 13.35 dB. Once again, the  $L=1$  and 2 cases are identical while the envelope detector has better performance when  $L=3$  or 4. This is true for the  $M$ -ary cases as well as for the Rayleigh and non-faded limits. These results agree with comparisons between envelope detectors and square-law detectors for detection of multiple-pulse radar signals [REF 11].

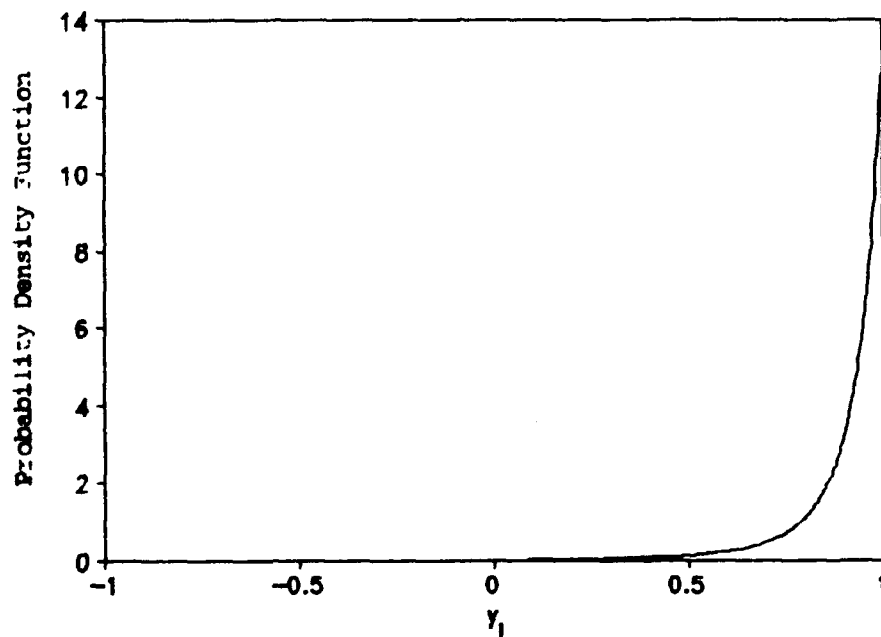


**Figure 4.31:  $f_{y_1}(y_1)$  where  $E_b/N_0=13.35\text{dB}$ ,  $E_b/N_j=20\text{dB}$ , Direct/Diffuse=10, and  $\gamma=.25$  with Square-Law Detection**

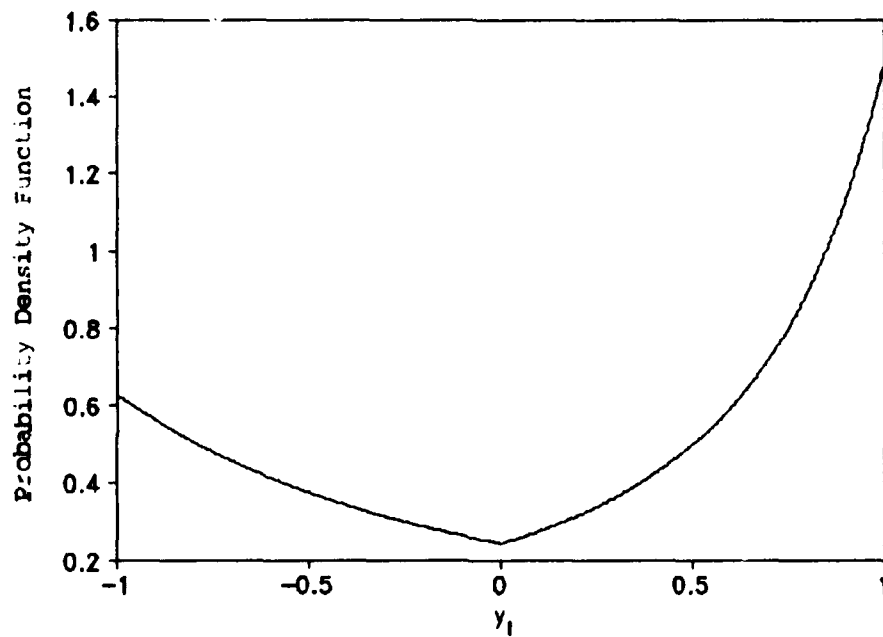


**Figure 4.32:  $f_{y_1}(y_1)$  where  $E_b/N_0=13.35\text{dB}$ ,  $E_b/N_j=3\text{dB}$ , Direct/Diffuse=10, and  $\gamma=.25$  with Square-Law Detection**

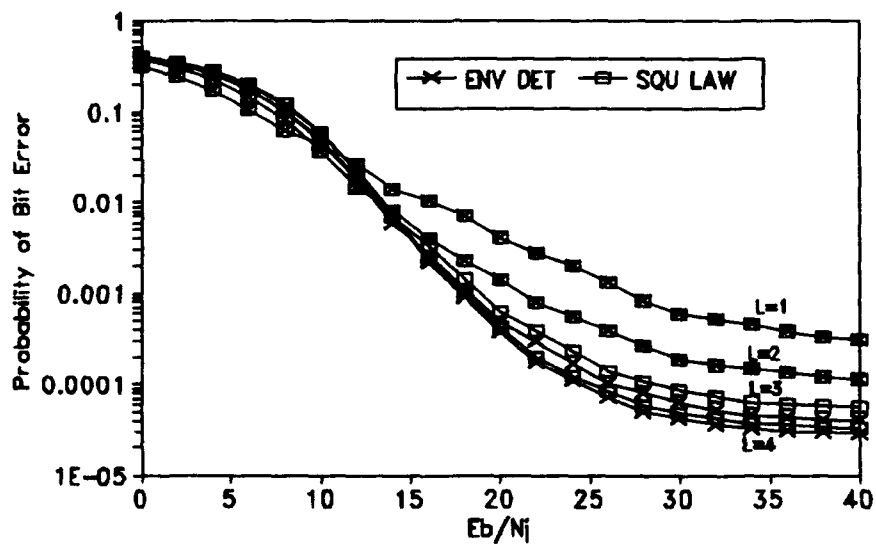


**Figure 4.33: Envelope Detector versus Square-Law Detector Worst Case Performance for BFSK Receivers where  $E_b/N_0=16\text{dB}$ , Direct/Diffuse=10**

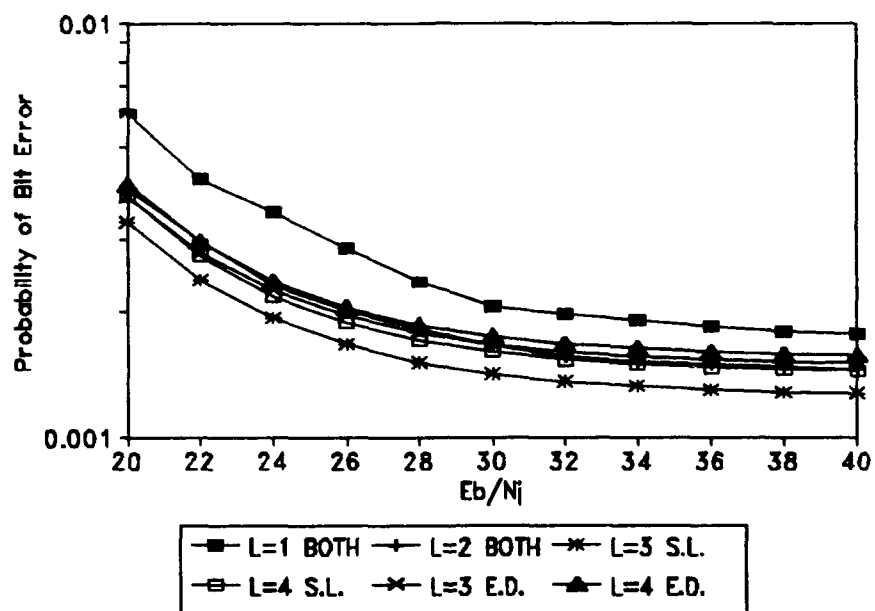


**Figure 4.34: Envelope Detector Performance versus Square-Law Detector Performance for BFSK Receivers where  $E_b/N_o=13.35\text{dB}$ , Direct/Diffuse=10**

## V. CONCLUSIONS

This thesis has presented an error probability analysis of a fast frequency-hopped, MFSK noncoherent receiver with ratio-statistic combining for a Rician channel with partial-band interference. The main focus of the thesis is the performance of ratio-statistic combining in the system. The thesis shows that ratio-statistic combining used in conjunction with diversity limits degradation due to fading and partial-band interference and generally provides an improvement in overall performance.

One conclusion of the thesis is that Rician fading and partial-band interference have a significant impact on receiver performance. The results show that the BFSK receiver performance varies by nearly three decades from the Rayleigh limit to the Gaussian limit. Also, the worst case performance of a BFSK receiver with ratio-statistic combining is much better at the Gaussian limit than at the Rayleigh limit.

The second conclusion of the thesis is that the ratio-statistic combining circuit provides protection from partial-band interference as diversity is increased. For a BFSK receiver where the direct-to-diffuse ratio is 10 and the signal-to-thermal noise ratio is 16 dB, the receiver degradation due to partial-band jamming is minimal for

diversities greater than four. It is very interesting to note that, for  $M$ -ary systems, the receiver is more sensitive to partial-band jamming than for binary systems and does not provide as much immunity at lower diversities even though the overall performance at higher signal-to-jammer ratios is better. The results illustrate this increased sensitivity, however, the effect is not in reality as depicted since the union bound is too loose to give correct results in the  $M$ -ary cases. As  $M$  increases, it is expected that the performance is better.

The third conclusion of the thesis involves a comparison of the performance of envelope detectors versus square-law detectors. The thesis proves analytically that, for no diversity, the performance of a receiver using envelope detection is identical to that of a receiver using square-law detection. For a diversity of two, the numerical results show that the performance of a receiver using envelope detection is still identical to that of a receiver using square-law detection for the specific parameters used, although, it can not be proven analytically. The results also show that, for diversities of three and four, the receiver using envelope detection performs better than that of a receiver using square-law detection. This is true for all cases examined in this thesis.

In general, the results show that, at lower signal-to-jammer ratios, diversity decreases the receiver performance.



As the signal-to-jammer ratio increases to 15 or 20 dB, diversity provides a significant amount of immunity to partial-band interference when the effects of thermal noise are negligible. The point where diversity should be used is dependent on thermal noise and fading.

One possible extension to this thesis would be to find a tighter bound for the  $M$ -ary case. As discussed in Chapter III, this requires obtaining a more general pdf than the one used in this thesis. One possible improvement would be to run a simulation to determine the tightness of the bound that is used.

## REFERENCES

1. A. C. Clarke, "Extraterrestrial Relays", *Wireless World*, vol. 51, no. 10, pp. 305-308, Oct. 1945.
2. C. M. Keller and M. B. Pursley, "Clipped Diversity Combining for Channels with Partial-Band Interference-Part II: Ratio-Statistic Combining," *IEEE Transactions on Communications*, vol. COM-37, no. 2, pp. 145-151, Feb. 1989.
3. Proakis, J. G., *Digital Communications*, 2nd Ed., New York: McGraw Hill, 1989.
4. Couch, Leon W., *Digital and Analog Communications*, New York: Macmillian Publishing Company, 1990.
5. Lathi, B. P., *Modern Digital and Analog Communication Systems*, 2nd Ed., Dryden Press, 1989.
6. Cooper, George R., and McGillem, Clare D., *Probabilistic Methods of Signal and Sytems Analysis*, 2nd Ed., Holt, Reinhart and Winston, 1971.
7. Papoulis, Athanasios., *Probability, Random Variables, and Stochastic Processes.*, 2nd Edition, McGraw Hill, 1984, pp. 141-147.
8. C. M. Keller and M. B. Pursley, "Diversity Combining for Channels with Fading and Partial-Band Interference," *IEEE Journal on Selected Areas in Communications*, vol. SAC-5, no. 2, pp. 248-260, Feb. 1987.
9. R. Clark Robertson and Tri T. Ha, "Error Probabilities of Frequency-Hopped FSK with Self-Normalization Combining in a Fading Channel with Partial-Band Interference,"
10. Gradshteyn, I. S. and Ryzhik, I. M., *Table of Integrals, Series, and Products, Corrected and Enlarged Edition*, translated and edited by Alan Jeffrey, New York: Academic Press, 1980.
11. Whalen, Anthony D., *Detection of Signals in Noise.*, Academic Press, 1971, pg. 263.
12. J. S. Lee, L. E. Miller and R. H. French, "The Analysis of Uncoded Performances for Certain ECCM Receiver Design Strategies for Multihops/Symbol FH/MFSK Waveforms," *IEEE Journal on Selected Areas in Communications*, vol. SAC-3, no. 5, Sep. 1985.

### INITIAL DISTRIBUTION LIST

- |   |   |
|---|---|
| 1. Defense Technical Information Center<br>Cameron Station<br>Alexandria, Virginia 22304-6145                                   | 2 |
| 2. Library, Code 52<br>Naval Postgraduate School<br>Monterey, California 93943-5002   | 2 |
| 3. Chairman Code EC<br>Department of Electrical and<br>Computer Engineering<br>Monterey, California 93943-5000                  | 1 |
| 4. Prof. R. C. Robertson, Code EC/Rc<br>Department of Electrical and<br>Computer Engineering<br>Monterey, California 93943-5000 | 5 |
| 5. Prof. T. T. Ha, Code EC/Ha<br>Department of Electrical and<br>Computer Engineering<br>Monterey, California 93943-5000        | 1 |
| 6. LT John F. Riley<br>Class 3-91B<br>Engineering Duty Officer School<br>Mare Island<br>Vallejo, California 94592-5018          | 2 |